Molecular Therapy
Original Article

Targeted Integration and High-Level Transgene Expression in AAVS1 Transgenic Mice after *In Vivo* HSC Transduction with HDAd5/35++ Vectors

Chang Li,[1] Arpit Suresh Mishra,[1] Sucheol Gil,[1] Meng Wang,[1] Aphrodite Georgakopoulou,[1] Thalia Papayannopoulou,[2] R. David Hawkins,[1] and André Lieber[1,3]

[1]Division of Medical Genetics, Department of Medicine, University of Washington, Box 357720, Seattle, WA 98195, USA; [2]Division of Hematology, University of Washington, Box 357720, Seattle, WA 98195, USA; [3]Department of Pathology, University of Washington, Box 357720, Seattle, WA 98195, USA

Our goal is the development of *in vivo* hematopoietic stem cell (HSC) transduction technology with targeted integration. To achieve this, we modified helper-dependent HDAd5/35++ vectors to express a CRISPR/Cas9 specific to the "safe harbor" adeno-associated virus integration site 1 (AAVS1) locus and to provide a donor template for targeted integration through homology-dependent repair. We tested the HDAd-CRISPR + HDAd-donor vector system in AAVS1 transgenic mice using a standard *ex vivo* HSC gene therapy approach as well as a new *in vivo* HSC transduction approach that involves HSC mobilization and intravenous HDAd5/35++ injections. In both settings, the majority of treated mice had transgenes (GFP or human γ-globin) integrated into the AAVS1 locus. On average, >60% of peripheral blood cells expressed the transgene after *in vivo* selection with low-dose O^6BG/bis-chloroethylnitrosourea (BCNU). *Ex vivo* and *in vivo* HSC transduction and selection studies with HDAd-CRISPR + HDAd-globin-donor resulted in stable γ-globin expression at levels that were significantly higher (>20% γ-globin of adult mouse globin) than those achieved in previous studies with a SB100x-transposase-based HDAd5/35++ system that mediates random integration. The ability to achieve therapeutically relevant transgene expression levels after *in vivo* HSC transduction and selection and targeted integration make our HDAd5/35++-based vector system a new tool in HSC gene therapy.

INTRODUCTION

Current hematopoietic stem cell gene therapies in patients use lentivirus vectors for gene delivery.[1,2] Lentivirus vectors efficiently integrate in the human genome with a strong bias toward actively transcribed genes. This semi-random integration pattern entails a risk of perturbing the expression of neighboring genes, including cancer-related genes. Therefore, a major goal in the field is to target transgene integration to a preselected site. A number of "safe harbors" for targeted integration into the human genome have been suggested (e.g., adeno-associated virus integration site 1 [AAVS1]).[3] Among the criteria for a safe harbor site are (1) a distance of more than 50 kb from the 5′ end of any gene, (2) a distance of >300 kb from cancer-related genes, (3) a distance of more than 300 kb from any microRNA, (4) a location outside of a gene transcription unit, and (5) a location outside of ultra-conserved regions. The AAVS1 locus on chromosome (chr)19 is used by wild-type AAV for integration mediated by the virus-encoded protein Rep78, which recognizes a specific motif (Rep-binding site [RBS]) within the AAVS1 site.[4,5] Because a large proportion of the human population has encountered AAV, as evidenced by detectable antibodies against some AAV serotypes, but without any discernable pathology, it was concluded that integration into AAVS1 may be safe.[6] Furthermore, this locus contains a DNase I hypersensitive site and an insulator that maintain an open chromatin conformation in $CD34^+$ and induced pluripotent stem cells (iPSCs).[7–9] This allows better access of genome editing tools and, on the other hand, should support high-level transgene expression.[7,10]

Targeted transgene integration can be achieved via homology-directed repair (HDR).[11] Following cleavage by an engineered site-specific nuclease, DNA double-strand breaks are resolved through non-homologous end joining (NHEJ), an error-prone DNA repair pathway that typically leads to variable insertions or deletions (indels), or HDR, which repairs DNA by copying a homologous donor template. Delivery of exogenous DNA flanked by DNA homologous to the genomic sequence around the break site can lead to incorporation of the exogenous sequence in a site-specific manner.

Current approaches to achieve targeted integration are based on electroporation of hematopoietic stem cells (HSCs) *in vitro* with endonuclease-encoding mRNA/ribonucleoproteins (RNPs) and donor plasmid DNA,[12–15] integration-deficient lentivirus vectors (IDLVs),[11,16] or rAAV6 vectors.[17–19] We developed helper-dependent adenovirus (HDAd5/35++) vectors to deliver designer

Received 21 May 2019; accepted 14 August 2019;
https://doi.org/10.1016/j.ymthe.2019.08.006.

Correspondence: André Lieber, Division of Medical Genetics, Department of Medicine, University of Washington, Box 357720, Seattle, WA 98195, USA.
E-mail: lieber00@uw.edu

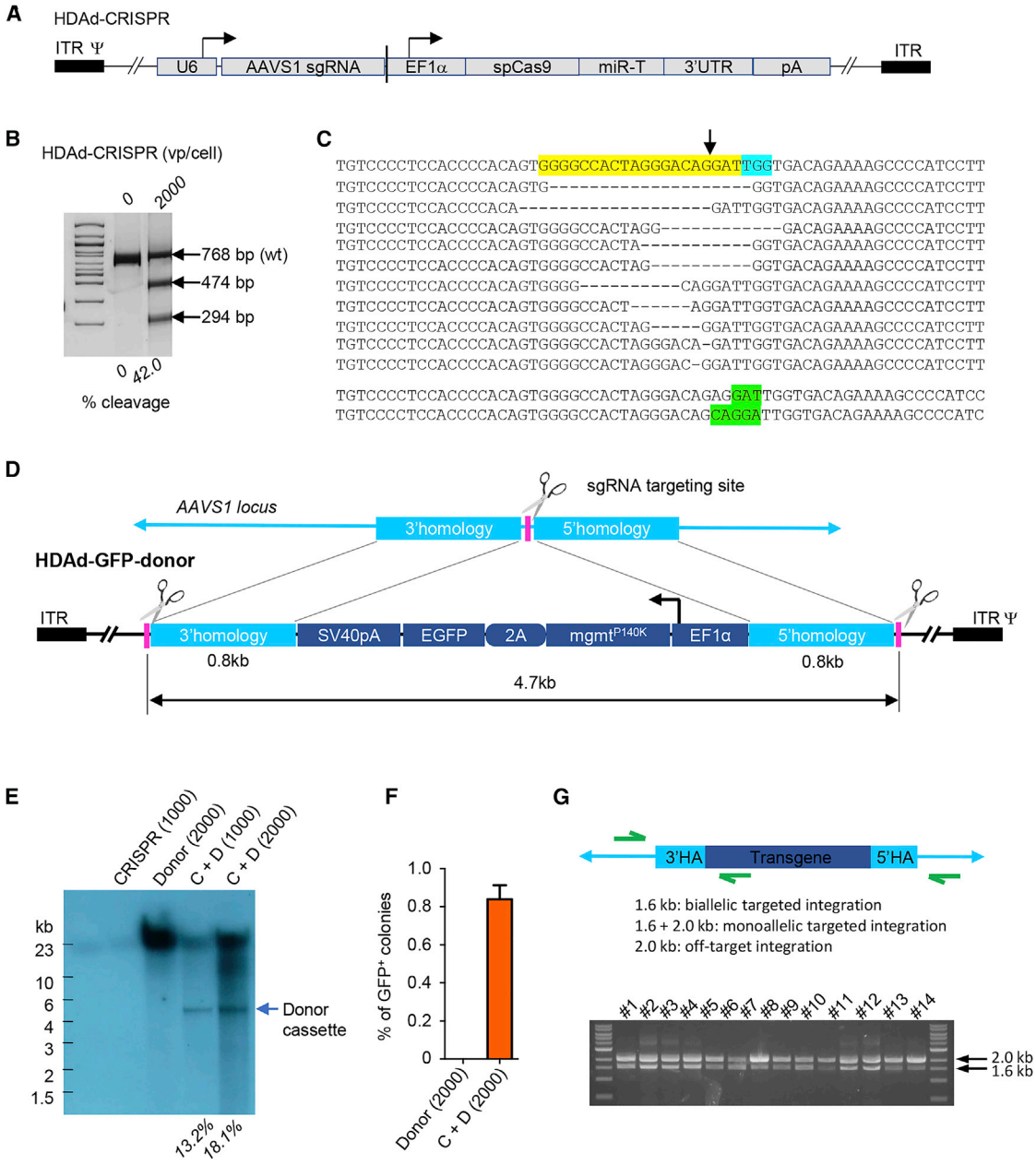

Figure 1. Characterization of the AAVS1-Specific CRISPR/Cas9 Vector and Donor Vector for HDR-Mediated Integration

(A) HDAd-CRISPR vector structure. The AAVS1-specific sgRNA is transcribed by PolIII from the U6 promoter, and the spCas9 gene is under control of the EF1α promoter. Cas9 expression is controlled by miR-183-5p and miR-218-5p, which suppress Cas9 expression in HDAd producer 116 cells but do not negatively affect Cas9 expression in CD34$^+$ cells.[21] The corresponding microRNA target sites (miR-Ts) were embedded into a 3′ UTR of the β-globin gene. (B) Target site cleavage frequency in human CD34$^+$ cells measured by T7E1 assay 3 days after HDAd-CRISPR transduction at a MOI of 2,000vp/cell. The specific cleavage products are 474 bp and 294 bp. The cleavage efficacy is shown below the gel. (C) The top 13 most frequent indels found in HDAd-CRISPR-transduced CD34$^+$ cells. The yellow sequence shows the target of the guide RNA, with the protospacer adjacent motif (PAM) sequence marked in blue. The CRISPR/Cas9 cleavage site is marked by a vertical arrow. Shown in green are insertions caused by NHEJ. (D) Structure of the donor vector for integration into the AAVS1 site (HDAd-GFP-donor). The mgmt^{P140K} gene is linked to the GFP gene through a self-cleaving picornavirus 2A peptide. The genes are under control of the EF1α promoter. pA, SV40 poly-adenylation signal. The transgene cassette is flanked by 0.8-kb regions of homology to the AAVS1 locus and are similar to a study published previously.[8] Upstream and downstream of the homology region are recognition sites for the AAVS1-specific CRISPR/Cas9 to release the donor cassette. (E) Release of the donor cassette. CD34$^+$ cells were infected with the HDAd-GFP-donor (D; at MOIs of 1,000 or 2,000 vp/cell) alone or in combination with HDAd-CRISPR (C; MOI of 1,000 vp/cell). Three days later, genomic DNA was subjected to Southern blot with a GFP-specific probe. The (linear) full-length HDAd-donor-GFP genome runs at ~31 kb. The released cassette runs at 4.7 kb. The cleavage frequency is shown below the gel. (F) Percentage of GFP-positive

(legend continued on next page)

integrases[20,21] and, in this study, donor templates. HDAd5/35++ vectors target human CD46, a receptor that is expressed on primitive HSCs.[22]

The ability of HDAd5/35++ vectors to efficiently deliver their genomes into the nucleus of non-dividing cells allows high amounts of donor DNA, a prerequisite for efficient targeted integration. Because HDAd5/35++ vectors can carry up to 30 kb of foreign DNA, they can accommodate long stretches of donor sequences that are homologous to the given target site. This should increase the efficacy of gene targeting by homologous recombination, which directly correlates with the length of the homology region.[23–27] Because these vectors are easy to produce at high yields and have strong HSC tropism, we employed them for *in vivo* HSC transduction.[22] The central idea of our approach is to mobilize HSCs from the bone marrow using granulocyte colony-stimulating factor (G-CSF)/AMD3100, and while they circulate at high numbers in the periphery, transduce them with an intravenously injected HDAd5/35++ vector. Transduced cells return to the bone marrow, where they persist long term. We have demonstrated the safety and efficacy of the approach in CD46 transgenic (tg) mouse models for hemoglobinopathies either by CRISPR/Cas9-mediated reactivation of endogenous fetal globin[20] or by fetal globin gene addition using a hyperactive Sleeping Beauty transposase (SB100x) that mediates efficient random transgene integration.[28] Although SB100x-mediated transgene integration is theoretically safer than quasi-random integration of lentivirus vectors, it still raises concerns regarding transgene silencing, undesired effects on neighboring genes, and genomic rearrangements. The goal of this study was therefore to modify our HDAd5/35++-based *in vivo* HSC transduction approach for targeted integration into AAVS1.

A sequence homologous to the human AAVS1 locus is absent in rodents.[29] Two tg rodent models have been reported previously that contain either a 3.5-kb fragment of the AAVS1 locus in the rat (7 head-to-tail copies) or mouse genome (X chromosome).[30] A study showed that the open chromatin structure of AAVS1 is maintained in tg mice.[31] The Jackson Laboratory distributes AAVS1 tg mice.[32] The Jackson Laboratory's website states that these mice contain five copies of an 8.2-kb human AAVS1 locus fragment inserted into a single genomic site. To make AAVS1 tg mice suitable for transduction with HDAd5/35++ vectors, we crossed them with mice that were tg for the human CD46 locus.[33] All animal studies were performed with AAVS1/CD46$^{+/+}$ mice.

Here we report a novel HDAd5/35++ vector system for targeted integration. We achieved efficient and high-level transgene expression in AAVS1 tg mice after *ex vivo* and *in vivo* HSCs transduction.

RESULTS

Design of HDAd-CRISPR and HDAd-Donor Vectors

We constructed a HDAd5/35++ vector expressing a CRISPR/Cas9 capable of creating double-stranded DNA (dsDNA) breaks within the AAVS1 locus (Figure 1A). Previous studies demonstrated that site-specific integration into this locus allowed robust transgene expression without side effects in primary human cells.[8] To test the activity of the corresponding HDAd-CRISPR vector, we transduced human CD34$^+$ cells, a cell fraction that is enriched for HSCs. AAVS1 site-specific cleavage on day 3 after infection with a frequency of ~42% was demonstrated by mismatch-sensitive nuclease T7E1 assay (Figure 1B). For deep sequencing of indels, we PCR-amplified an ~250-bp region surrounding the predicted AAVS1 cleavage site and sequenced the products using an Illumina system (Figure 1C). 80% of indels were deletions ranging from 1–20 bp, and only 10% were 1- to 2-bp micro-insertions.

We used, for the first time, a HDAd5/35++ vector as donor vector. The first HDAd-donor vector contained an expression cassette for GFP and O-6-methylguanine-DNA methyltransferase (mgmt)^{P140K} flanked on both sides by 0.8-kb-long regions that are homologous to areas immediately adjacent to the CRISPR/Cas9 target site (Figure 1D). Linear double-stranded adenoviral genomes are covalently linked with the virus-produced "terminal protein" (TP) when they enter cells and are translocated to the nucleus.[34] The same is the case for HDAd5/35++ genomes, where the TP is helper virus derived. A previous study has shown that cleavage of transgene donors in the context of plasmids promotes nuclease-mediated targeted integration.[35] We therefore incorporated the single guide RNA (sgRNA) target sites for the AAVS1 CRISPR into the donor vector flanking the donor transgene cassette (Figure 1D). Co-infection of HDAd-CRISPR and HDAd-GFP-donor should therefore simultaneously create dsDNA breaks in the chromosomal AAVS1 target site and release the donor cassette from the incoming HDAd-donor genome inside the nucleus. We demonstrated HDAd-CRISPR-mediated release of the donor cassette from a co-infected HDAd-GFP-donor vector with an efficacy of 13.2% and 18.1% in CD34$^+$ cells on day 2 after infection at a total MOI of 1,000 and 2,000 viral particles (vp)/cell, respectively (Figure 1E). This finding also indicates that CRISPR/Cas9 is capable of cleaving double-stranded linear adenoviral DNA, which has implications for anti-viral therapies. Notably, because our donor vectors contained CRISPR/Cas9 cleavage sites, it was impossible to generate a vector that contained both the donor cassette and the CRISPR/Cas9 expression cassette.

Targeted Integration *In Vitro*

We transduced human CD34$^+$ cells with HDAd-GFP-donor + HDAd-CRISPR or HDAd-GFP-donor alone and plated transduced cells for a colony-forming unit (CFU) assay. On day 14 after plating,

colonies. Two days after transduction with HDAd-GFP-donor alone (MOI = 2,000 vp/cell) or together with HDAd-CRISPR (MOI = 1,000 vp/cell for each virus), cells were plated for the CFU assay. Fourteen days after plating, GFP-positive colonies were counted and analyzed for GFP expression. (G) In and out PCR analysis of the GFP-positive colonies. The top diagram shows the location of primers. Expected product sizes for various integration patterns are listed. The bottom gel pictures demonstrate that all clones had monoallelic targeted integration. C + D, CRISPR + donor.

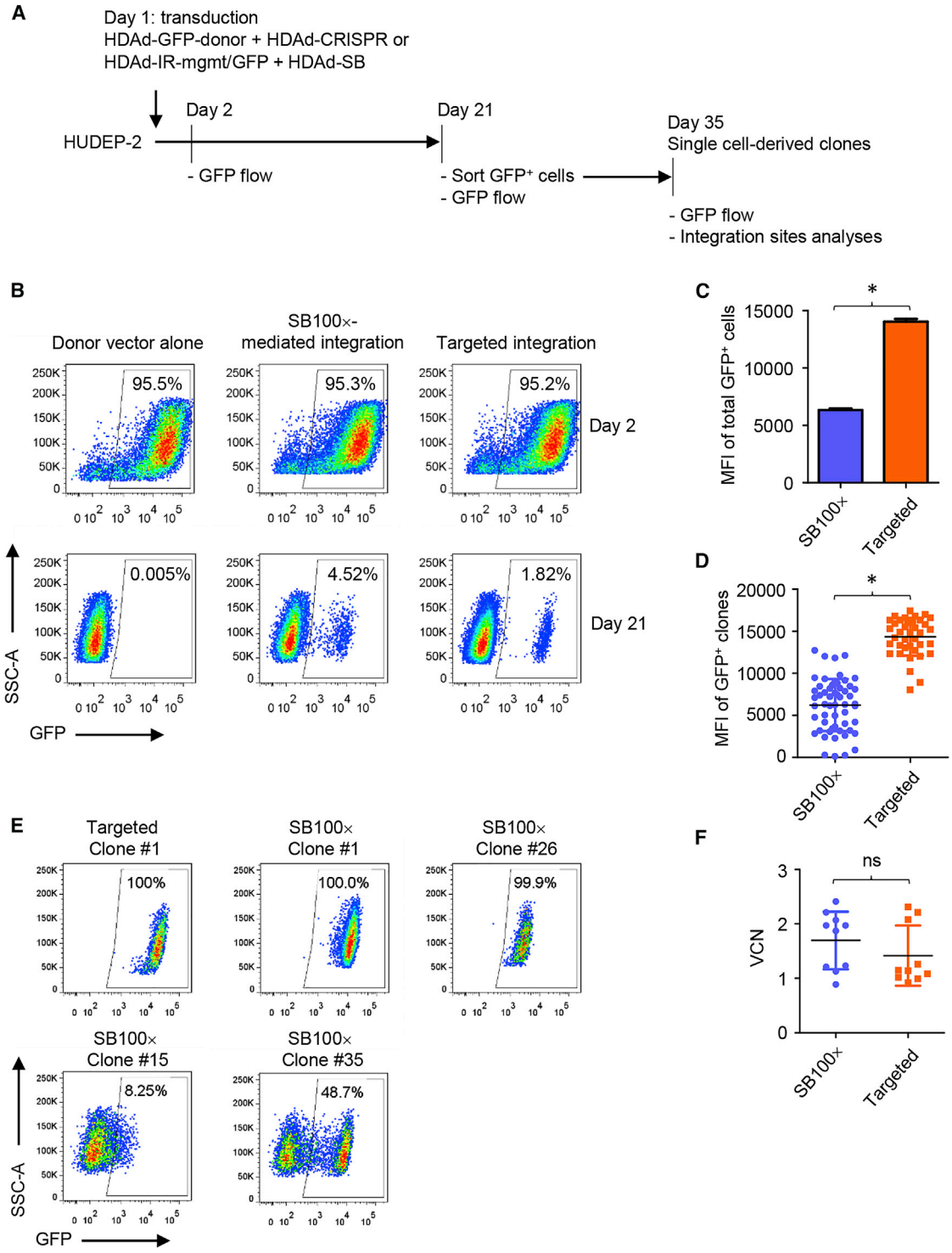

Figure 2. AAVS1-Targeted Integration versus Random SB100x-Mediated Integration in HUDEP-2 Cells

(A) Experimental scheme. HUDEP-2 cells were transduced with the indicated HDAd vectors at a MOI of 1,000 vp/cell for each virus. After expansion for 21 days, GFP-positive cells were sorted into a 96-well plate. Single cell-derived clones were obtained by further expansion for 2 weeks. GFP expression was measured on days 2 and 21 post-transduction in the cell population or on day 35 in cell clones. (B) GFP flow cytometry in cells treated with the donor vector alone or vectors with targeted versus SB100x

(legend continued on next page)

~0.9% of total colonies exhibited bright and uniform GFP expression (Figure 1F). Cells transduced with HDAd-GFP-donor alone did not give rise to colonies stably expressing GFP. We then performed a vector integration analysis in single GFP-positive colonies. Because of the long homology regions flanking the transgene cassette, it was not possible to employ commonly used tools for vector integration site analysis (e.g., linear-amplification mediated PCR [LAM-PCR]). To demonstrate the presence of vector-cellular DNA junctions, we used an inverse PCR (iPCR) method that involves the endonuclease cleavage of genomic DNA (gDNA) into ~4-kb fragments, their circularization, and subsequent PCR with transgene-specific primers.[6] The results showed that all 14 tested colonies had monoallelic targeted integration (Figure 1G). No off-target integration was detected. These data demonstrate the functionality of our vector system design in human cells.

We then tested our HDAd-CRISPR + HDAd-donor vector system for targeted integration *in vitro* in direct comparison with the SB100x vector system that mediates random integration (Figure 2A). We used HUDEP-2 cells, an immortalized human erythroid precursor cell line.[36] This cell line allows the expansion of single colonies, features that facilitate integration site analysis. GFP flow cytometry performed on day 2 after transduction of HUDEP-2 cells demonstrated similar percentages of GFP-positive cells for the SB100x-mediated and targeted integration systems, indicating similar transduction rates (Figure 2B, top panel). GFP expression on day 2 is likely to originate from episomal vector genomes because transduction with HDAd-GFP-donor alone resulted in similar GFP marking. After culturing transduced cells for 21 days, because of cell proliferation, episomal vector genomes nearly disappeared, as indicated by the absence of GFP expression in the HDAd-GFP-donor-alone setting. On day 21, 4.52% and 1.82% of cells were GFP-positive for the SB100x-mediated and targeted integration system, respectively (Figure 2B, bottom panel). This suggests that the SB100x system confers higher stable transduction rates. However, the level of GFP expression, reflected by the mean fluorescence intensity (MFI), was higher in cells transduced with HDAd-CRISPR + HDAd-GFP-donor both in the cell population on day 21 (Figure 2C) and at the single-clone level (Figure 2D). Integration analysis by in and out PCR showed that all tested 36 colonies derived from HDAd-CRISPR + HDAd-GFP-donor-transduced HUDEP-2 cells had transgenes integrated into the AAVS1 site (Figure S1A). Sequencing of amplicons showed that, in all clones except clone 20 Figures S1A and S1C, integration occurred through HDR. This is in line with the homogeneous high level of transgene expression in clones with targeted integration. Figure S1B shows the integration pattern of clone #20. In and out PCR with AAVS1 and transgene-specific primers revealed that integration in 3 of 36 colonies occurred in both alleles; 31 of 36 had monoallelic integrations (Figure S1C). The additional smaller bands in clones 17 and 36 resulted from deletions within the multiple-copy AAVS1 locus (Figures S1D and S1E). In contrast, SB100x-mediated random integration with no preferential targeting of a specific locus[28,37] resulted in varying levels of gene silencing (Figure 2E). Similar levels of vector copy numbers were detected in clones with SB100x and targeted integration (Figure 2F).

In summary, the *in vitro* studies showed that the HDAd-CRISPR + HDAd-GFP-donor system conferred targeted integration with high efficiency and resulted in higher GFP expression levels than the SB100x-mediated system. The efficacy of stable integration was ~40% lower for the targeted system.

Ex Vivo Transduction of AAVS1/CD46 HSCs with HDAd-CRISPR + HDAd-GFP-Donor and Subsequent Transplantation into Lethally Irradiated Recipients

We next tested our targeted integration system in HSCs AAVS1/CD46-tg mice. The target site cleavage frequency after *ex vivo* transduction of lineage-negative (Lin^-) cells, a bone marrow cell fraction enriched for HSCs, was ~25% after transduction with the HDAd-CRISPR vector at a MOI of 1,000 vp/cell (Figure S2). We chose a total MOI of 500 vp/cell for *ex vivo* transduction experiments to minimize potential adverse effects associated with high-level CRISPR/Cas9 expression[38] while maintaining efficient cleavage activity. AAVS1/CD46 Lin^- cells transduced *ex vivo* with HDAd-CRISPR alone (MOI = 500 vp/cell), HDAd-GFP-donor alone (MOI = 500 vp/cell), and a combination of both (MOI = 250 vp/cell for each vector) were transplanted into lethally irradiated C57BL/6 mice, which were then followed for 16 weeks (Figure 3A). Donor cell engraftment rates were comparable for all three settings (Figure S3), suggesting that the genomic modification introduced in HSCs by the HDAd-CRISPR and HDAd-CRISPR + HDAd-GFP-donor vectors had no detrimental effects on HSC biology, specifically on the multilineage repopulation of lethally irradiated recipients. GFP marking rates reaching up to 100% appeared in peripheral blood mononuclear cells (PBMCs) after three rounds of O^6BG/bis-chloroethylnitrosourea (BCNU) selection of HSCs and progenitors that stably expressed transgenes (Figures 3B and 3C). Before selection (4 weeks after transplantation), the percentage of GFP-positive PBMCs was, on average, 1.1%, indicating that targeted integration is a rare event. GFP-positive PBMCs were less than 0.2% on average in mice that were transplanted with Lin^- cells transduced with HDAd-GFP-donor only. This points toward the necessity of CRISPR/Cas9-mediated dsDNA breaks to achieve stable transgene expression. Mice analyzed at week 16 after transplantation showed GFP marking in all lineages analyzed in bone marrow, spleen, and PBMCs (Figure 3D). GFP marking rates were maintained for 16 weeks in secondary transplant recipients, demonstrating that primitive HSCs were genetically modified with the HDAd-CRISPR + HDAd-GFP-donor vector system (Figure S4).

integration mechanisms on days 2 and 21. (C) Mean fluorescence intensity of GFP in total GFP-positive cells with targeted versus SB100x integration (day 21). Data shown (mean ± SD) represent three independent experiments. *$p < 0.05$. (D) Mean fluorescence intensity of GFP in single clones. Each symbol represents an individual cell clone. Data shown (mean ± SD) are representative of two independent experiments. *$p < 0.05$. (E) Flow cytometry showing GFP expression in representative cell clones with targeted or SB100x-mediated integration. (F) Vector copy number in cell clones measured by qPCR using GFP primers. ns, not significant.

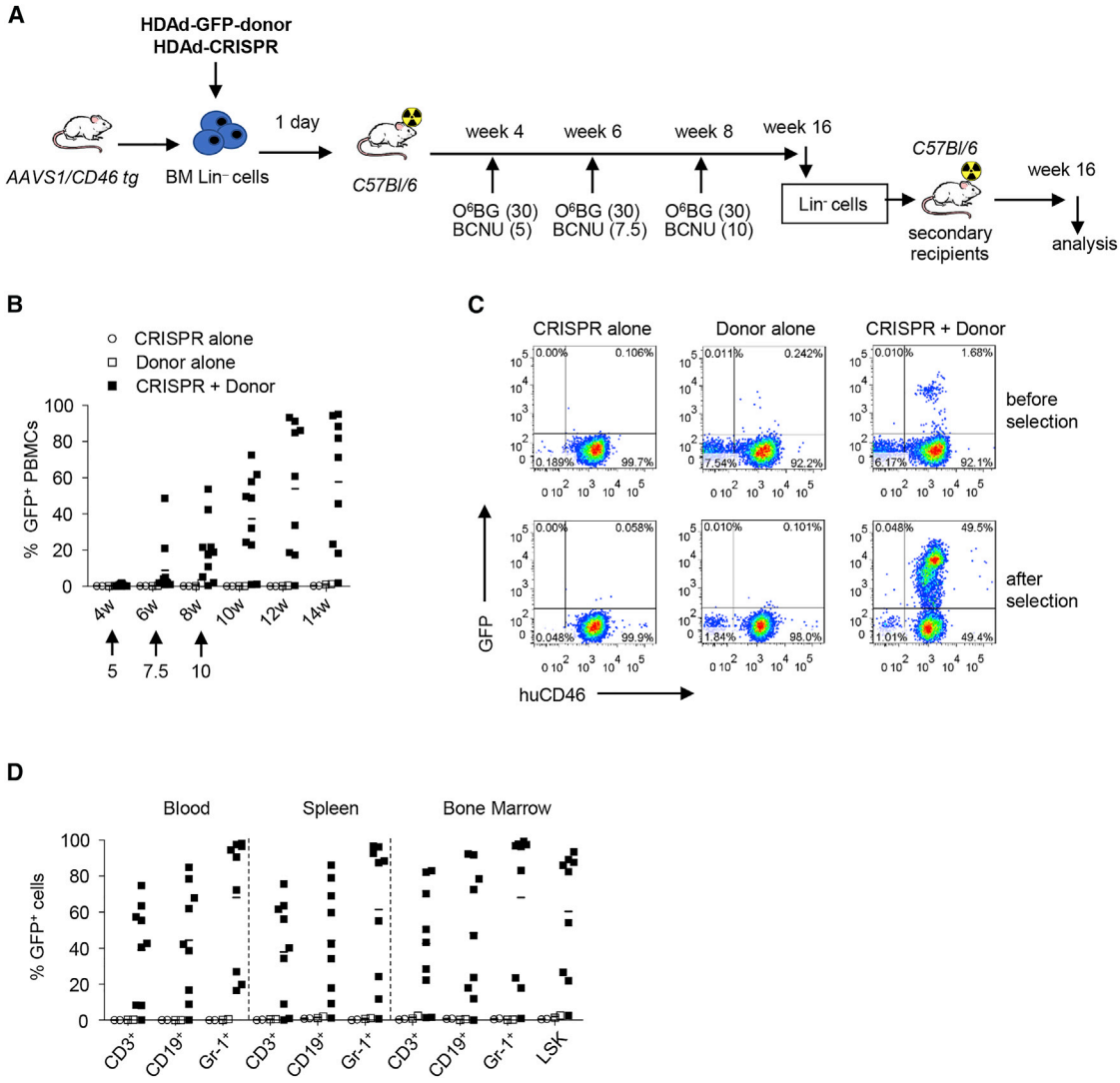

Figure 3. *Ex Vivo* Transduction of AAVS1/CD46 Lin⁻ Cells with HDAd-CRISPR and HDAd-GFP-Donor and Subsequent Transplantation into Lethally Irradiated Recipients

(A) Schematic of the experiment. Bone marrow was harvested from AAVS1/CD46-tg mice and lineage-negative (Lin⁻) cells were isolated by MACS. Lin⁻ cells were transduced with HDAd-CRISPR and HDAd-GFP-donor alone or in combination at a total MOI of 500 vp/cell. After 1 day in culture, 1×10^6 transduced cells/mouse were transplanted into lethally irradiated C57BL/6 mice. At week 4, O^6BG/BCNU treatment was started and repeated two times every 2 weeks. With each cycle, the BCNU concentration was increased, from 5 mg/kg to 7.5 mg/kg to 10 mg/kg. At week 16, mice were sacrificed, and bone marrow Lin⁻ cells were used for transplantation into lethally irradiated secondary C57BL/6 recipients, which were then followed for 16 weeks. (B) Percentage of GFP-positive cells in peripheral blood mononuclear cells (PBMCs), measured by flow cytometry. Shown are groups that were transplanted with Lin⁻ cells transduced with HDAd-CRISPR only, HDAd-GFP-donor only, and HDAd-CRISPR + HDAd-GFP-donor. Each symbol represents an individual animal. N = 3 for CRISPR only, N = 3 for donor only, N = 10 for CRISPR + donor. $p < 0.01$ for CRISPR + donor versus CRISPR only and donor only for all time points after week 6. In mice that were transplanted with mock-transduced Lin⁻ cells, less than 0.1% of cells were GFP-positive. (C) Percentage of GFP-positive cells in PBMCs from representative mice transplanted with Lin⁻ cells. Data from week 4 (before selection) and week 12 (after selection) are shown. (D) Percentage of GFP-positive cells in lineage-positive $CD3^+$ cells (T cells), $CD19^+$ cells (B cells), Gr-1^+ cells (myeloid cells), and HSCs (LSK cells).

In Vivo HSC Transduction of AAVS1/CD46-tg Mice with HDAd-CRISPR + HDAd-GFP-Donor

Our main focus is the development of *in vivo* HSC transduction technology with targeted integration. For *in vivo* HSC transduction of AAVS1/CD46-tg mice, HSCs were mobilized from the bone marrow into the peripheral blood stream by subcutaneous injections of G-CSF/AMD3100 and transduced *in vivo* by intravenously delivered HDAd-CRISPR + HDAd-GFP-donor vectors (Figure 4A). After *in vivo* selection with three cycles of O^6BG/BCNU, ~60% of mice showed GFP expression in PBMCs ranging from 35% to 95% GFP-positive PBMCs in individual animals (Figure 4B). At week 14 after *in vivo* transduction, similar marking was seen in mononuclear cells

in the blood, spleen, and bone marrow (Figure 4C). GFP marking was seen in $CD3^+$, $CD19^+$, and $Gr\text{-}1^+$ lineage cells in the blood, spleen, and bone marrow (Figure 4D). In the bone marrow of "responders," more than 50% of $Lin^-/Sca1^+/cKit^+$ (LSK) cells (a fraction that is enriched for HSCs) were GFP positive (Figure 4D, last group). This was also reflected by a functional assay for HSCs and the ability to form progenitor colonies (Figure 4E). Furthermore, transduction of primitive, long-term repopulating HSCs was shown in secondary recipients (Figure S5). The *in vivo* HSC transduction and selection procedure had no negative influence on bone marrow cell composition and hematopoiesis (Figure 4F).

Ex Vivo and *In Vivo* HSC Transduction with the HDAd-CRISPR and HDAd-Globin-Donor Vector

Although studies with the HDAd-GFP-donor vector suggest stable HSC transduction in the majority of animals, a higher rate of responders would be desirable. This would require increasing the efficacy of HDR-mediated integration, which can be achieved by increasing the length of the homology arms.[23–25] We therefore generated a new HDAd-donor vector with 1.8-kb regions that were homologous to AAVS1 genomic sequences surrounding the CRISPR/Cas9 cleavage site (Figure 5A). For potential application in gene therapy of hemoglobinopathies, we used the human γ-globin gene (HBG1) under control of a mini-β-globin locus control region (LCR). We tested this HDAd-globin-donor vector both in the *ex vivo* and *in vivo* HSC transduction protocols. In the *ex vivo* transduction setting (Figure 5B), we observed that all mice responded, with 4 of 5 mice expressing γ-globin in 80% of peripheral red blood cells (RBCs) (Figure 5C). The percentage of γ-globin-positive erythroid ($Ter119^+$) cells in the blood and bone marrow was significantly higher than that of non-erythroid ($Ter119^-$) cells (Figure 5D). The same was the case for the γ-globin MFI (Figure 5E). This suggests that the mini-LCR confers preferential expression in erythroid cells. At week 16, the level of γ-globin was 20.52% (±5.66%) of that of adult mouse β-globin, as measured by high-performance liquid chromatography (HPLC) (Figure 5F), and 22.33% (±6.21%) by qRT-PCR (Figure 5G). In a previous study, performed under the same regimen with the SB100x system, γ-globin expression levels were 15.74% (+±2.69%) by HPLC and 15.40% (±9.21%) by qRT-PCR.[39] This implies that the level of γ-globin expression is higher for the targeted integration system compared with the SB100x system. In fact, for the targeted integration system, it would be in the range of curative levels, which is thought to be 20% γ-globin of adult globin for patients with β_0/β_0-thalassemia or sickle cell disease.[28] In agreement with previous studies,[28] we measured, in single Lin^- cell-derived colonies, on average, two integrated vector copies per genome at week 16 (Figure 5H). *Ex vivo* HSC transduction of Lin^- cells did not affect their ability for multilineage engraftment and complete hematopoietic reconstitution in lethally irradiated recipients (Figure S6). Analysis of secondary HSC transplant recipients showed that *ex vivo* transduction with the HDAd-CRISPR + HDAd-globin-donor vector followed by *in vivo* selection did not affect the pool of HSCs capable of long-term repopulation (Figure S7).

In the *in vivo* HSC transduction studies with the HDAd-CRISPR + HDAd-globin-donor vector (Figure 6A), after *in vivo* selection, 4 of 5 mice showed stable γ-globin expression in RBCs, ranging from 40% to 97% $\gamma\text{-globin}^+$ RBCs in individual mice (Figure 6B). γ-Globin expression was found preferentially in erythroid cells (Figures 6C and 6D). The γ-globin expression levels in RBCs were 23.97% (±7.22%) by HPLC (Figure 6E) and 24.53% (±7.34%) by qRT-PCR (Figure 6F) of that of adult mouse β-globin. The vector copy number per cell ranged from 1.5 to 2.5 in individual mice. In the same *in vivo* HSC transduction and selection setting, using the SB100x-based γ-globin vectors, γ-globin levels were 10.5% (±3.1%) by HPLC and 12.17% (±3.38%) by qRT-PCR, with an average of 2 integrated vector copies per genome (Figure 6G).[28] The composition of lineage-positive cells in the blood, spleen, and bone marrow and LSK cells in bone marrow at week 16 after *in vivo* transduction was normal (Figure 6H). Transplantation of bone marrow Lin^- cells harvested at week 16 after *in vivo* transduction with HDAd-CRISPR + HDAd-globin-donor into lethally irradiated recipients showed 100% engraftment and stable γ-globin expression in RBCs over 16 weeks, with an average γ-globin level of 24% of that of adult β-globin (Figure S8).

In summary, our HSC transduction studies with HDAd-CRISPR + HDAd-globin-donor resulted in stable γ-globin expression at levels that are significantly higher than those achieved in previous studies with the SB100x-based system. Clearly, to conclude that this is the result of targeted integration into AAVS1 (which has an open chromatin profile) requires integration site analysis in bone marrow cells of transduced AAVS1/CD46-tg mice.

Localization of the AAVS1 Locus in AAVS tg Mice

iPCR for integration site analysis requires knowledge of AAVS1 locus localization in the genome of AAVS1/CD46-tg mice. To determine this, we used targeted locus amplification (TLA)-PCR technology that involves crosslinking of physically proximal sequences[40] (Materials and Methods). The TLA data obtained from bone marrow cells from AAVS1/CD46-tg mice were then aligned with a reference mouse genome. The TLA results indicate that the AAVS1 transgene is integrated into chr14 at the location (chr14:110443871–110461834), accompanied by an 18-kb deletion of the mouse genome sequence (Figure 7A). Using this information, we then used primers to amplify and sequence into the locus (Figure 7B). We found repeats of the AAVS1 locus facing left to right and right to left. Both terminal repeats (1 and 5) were truncated and 4.5 and 2.8 kb long, respectively. Repeat 5 lacked a complete 5′ homology region. This constellation of target sites complicated the integration site analysis. Some of the theoretical outcomes for integration by the HDAd-CRISPR + HDAd-donor system are outlined in Figure S9.

Chromosomal Integration after *Ex Vivo* and *In Vivo* HSC Transduction with HDAd-CRISPR+HDAd-Donor

First we performed a genomic Southern blot on DNA from bone marrow cells harvested at week 16 (Figure 8). Hybridization of EcoRI-digested gDNA with an AAVS1-specific probe showed, in all analyzed mice, a 3.9-kb-specific band indicative of integration of

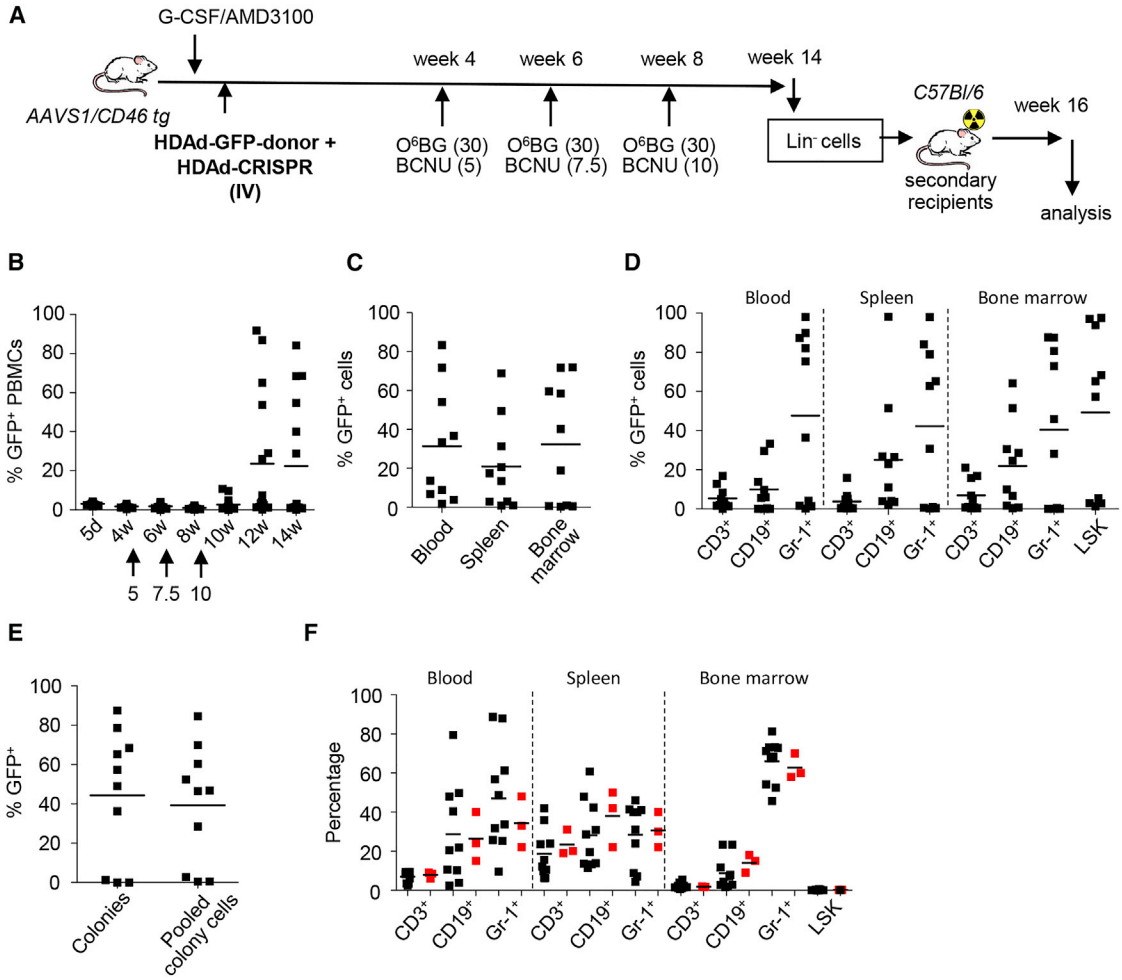

Figure 4. *In Vivo* Transduction of AAVS1/CD46-tg Mice with HDAd-AAVS1-CRISPR + HDAd-GFP-Donor

(A) Treatment regimen. AAVS1/hCD46tg mice were mobilized and injected intravenously (i.v.) with HDAd-CRISPR + HDAd-GFP-donor (twice, each 4×10^{10} vp of a 1:1 mixture of both viruses). Four weeks later, O^6BG/BCNU treatment was started. With each cycle, the BCNU concentration was increased from 5 mg/kg to 7.5 mg/kg and 10 mg/kg. The O^6BG concentration was 30 mg/kg for all three treatments. Mice were followed until week 14, when animals were sacrificed for analysis and Lin^- cell transplantation into secondary recipients. Secondary recipients were then followed for 16 weeks. (B) Percentage of GFP-positive cells in PBMCs, measured by flow cytometry. N = 13. The percentage of GFP-positive cells in mice that were mock-injected was less than 0.1%. (C) Percentage of GFP-positive cells in PBMCs, spleen, and bone marrow at week 14. (D) Percentage of GFP-positive cells in lineage-positive $CD3^+$ cells (T cells), $CD19^+$ cells (B cells), Gr-1^+ cells (myeloid cells), and HSCs (LSK cells). (E) Analysis of GFP-positive colonies. Total bone marrow Lin^- cells from week 14 mice were plated, and GFP expression in colonies was analyzed 12 days later. Each symbol is the average GFP-positive colony number for an individual mouse (left panels). Cells from all colonies were pooled and analyzed by flow cytometry (right panels). (F) Percentage of lineage-positive and LSK cells at week 14. Data from mock *in vivo*-transduced mice are shown as red symbols. The difference between mock and treatment groups was not significant.

the donor cassette into one (or more) repeats of the AAVS1 locus (Figure 8A). Hybridization of *BlpI*-digested DNA with the GFP probe resulted in 5.8-kb signals in 5 of 10 mice, representative of integration into the repeat 5-containing-only partial 5′ homology region (Figure 8B). The signals of other size could be the result of integration into repeats 1–4. Two of ten mice appeared to have integrations into several AAVS1 motif repeats. To demonstrate the presence of transgene-chromosome junctions, we performed iPCR on gDNA from mice (Figures 9A and 9B). Six of eight mice analyzed displayed PCR products consistent with HDR-mediated integration into the AAVS1 site (Figure 9B, green arrows). Several of these mice had additional bands that resulted from integration into one of the CRISPR/Cas9 off-target sites on ch5 (Figure 9B, red arrows). We also found bands that originated from integration of the full-length HDAd genome involving the inverted terminal repeats (ITRs) as junctions. Interestingly, these integrated full-length HDAd vector genomes were on chr14, the chromosome containing the CRISPR AAVS1 target site (Figure 9B, blue arrows). In an attempt to de-complex these results derived from a pool of bone marrow cells, we plated GFP-positive bone marrow Lin^- cells to generate progenitor colonies derived

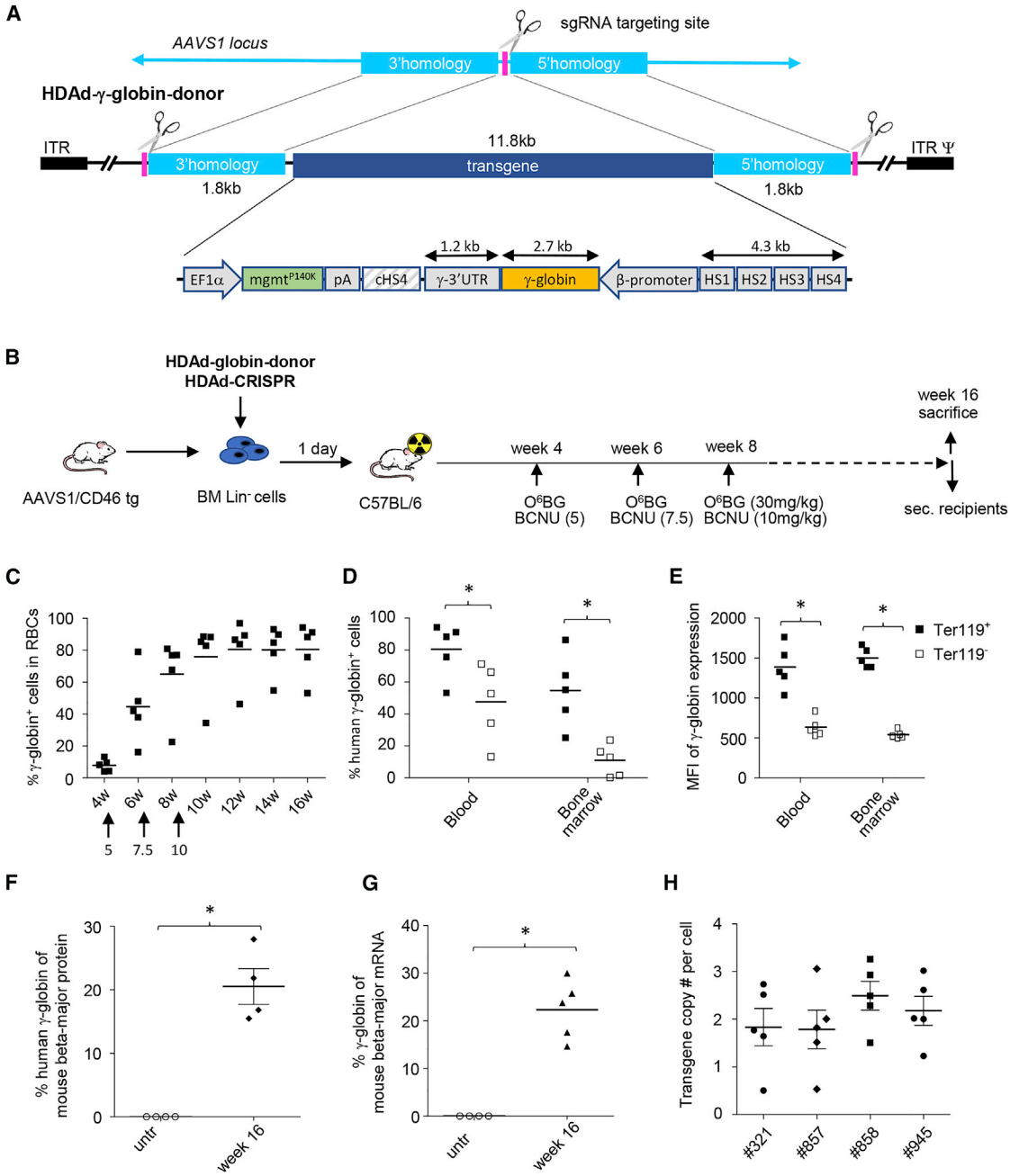

Figure 5. *Ex Vivo* Transduction of AAVS1/CD46 Lin⁻ Cells with HDAd-AAVS1 and HDAd-γ-Globin-Donor Vectors and Subsequent Transplantation into Lethally Irradiated Recipients

(A) Structure of the donor. The overall structure is the same as for the HDAd-GFP-donor vector (Figure 1D). The regions of homology are longer (1.8 kb versus 0.8 kb) in the new HDAd-globin-donor vector. The γ-globin expression cassette contains a 4.3-kb version of the β-globin LCR consisting of four DNase hypersensitivity (HS) regions and the β-globin promoter.[59] The full-length γ-globin cDNA, including the 3′ UTR (for mRNA stabilization in erythrocytes), was used. The mgmt^{P140K} gene is under control of the ubiquitously active EF1α promoter. The bi-directional SV40 poly-adenylation signal is used to terminate transcription. To avoid interference between the LCR/β-promoter and EF1α promoter, a 1.2-kb chicken HS4 chromatin insulator[60] was inserted between the cassettes. (B) The treatment regimen is the same as shown in Figure 3A. (C) Percentage of human γ-globin-positive cells in peripheral red blood cells (RBCs), measured by flow cytometry. In mice that were transplanted with mock-transduced Lin⁻ cells, less than 0.1% of cells were γ-globin positive. N = 5. (D and E) Percentage (D) and mean fluorescence intensity (E) of human γ-globin-positive cells in erythroid (Ter119$^+$) and non-erythroid (Ter119$^-$) cells in blood and bone marrow at week 16 after *in vivo* transduction. *p < 0.05. (F) Percentage of γ-globin chains relative to mouse β-major chains measured in RBCs at week 16 by HPLC. *p < 0.05. (G) Percentage of γ-globin mRNA relative to mouse β-major RNA measured in RBCs at week 16 by qRT-PCR. *p < 0.05. (H) Vector copy number per cell in colonies derived from Lin⁻ cells. Each symbol represents one colony. Differences between animals are not significant.

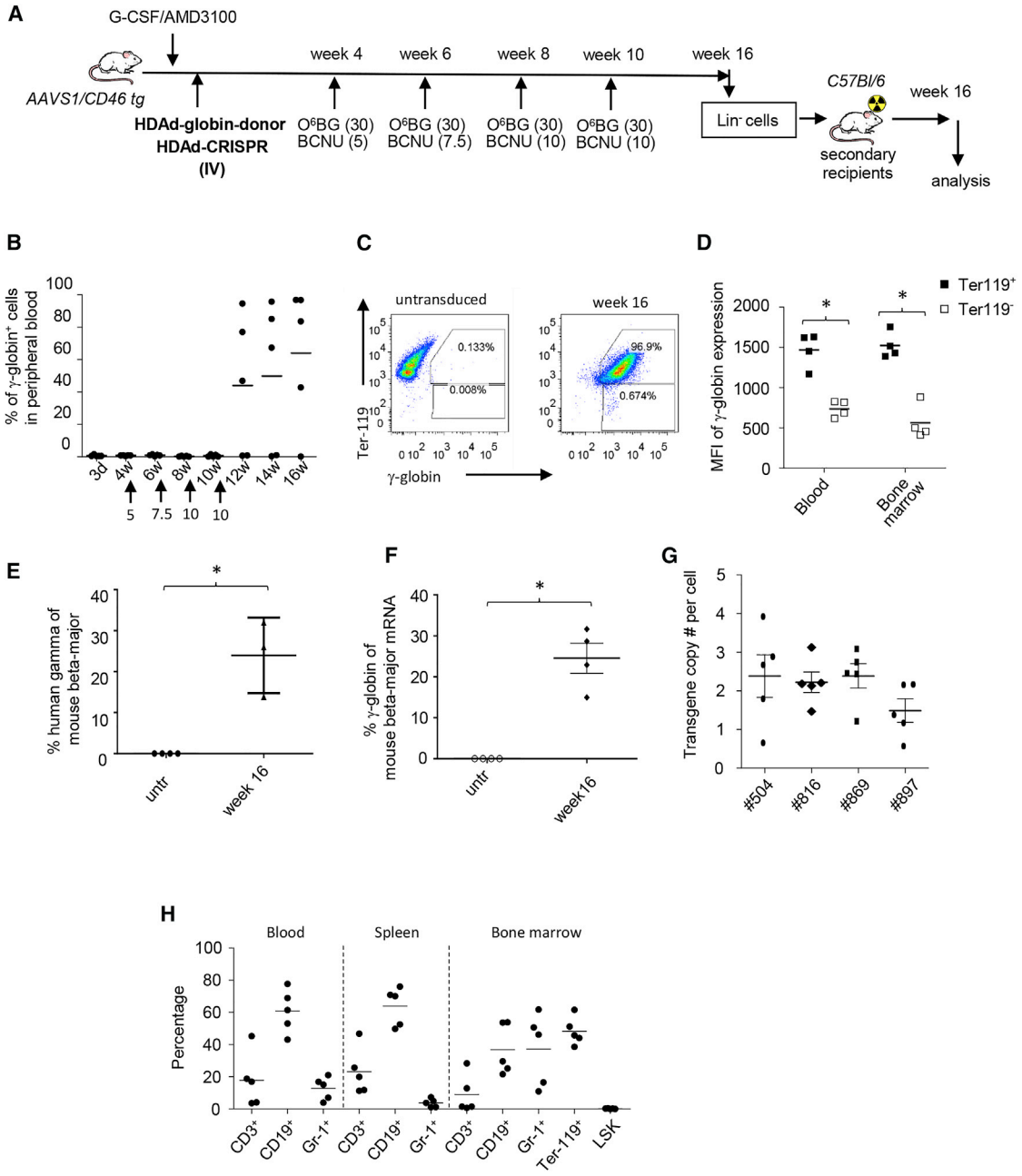

Figure 6. *In Vivo* Transduction of AAVS1/CD46-tg Mice with HDAd-CRISPR + HDAd-γ-Globin-Donor

A) Treatment regimen. (B) Percentage of γ-globin-positive RBCs. The percentage of γ-globin-positive cells in mice that were mock-injected was less than 0.1%. N = 5. (C) Representative flow cytometry analysis showing the percentage of γ-globin-positive cells in peripheral RBCs from untransduced control mice or mice at week 16 after *in vivo* transduction. (D) Mean fluorescence intensity of γ-globin in erythroid (Ter119$^+$) and non-erythroid (Ter119$^-$) cells in blood and bone marrow. *$p < 0.05$. (E) Percentage of γ-globin chains relative to mouse β-major chains measured in RBCs at week 16 by HPLC. *$p < 0.05$. (F) Percentage of γ-globin mRNA relative to mouse β-major RNA measured in RBCs at week 16 by qRT-PCR. *$p < 0.05$. (G) Vector copy number per cell in colonies derived from Lin$^-$ cells from four responder mice. Each symbol represents one colony. Differences between animals are not significant. (H) Composition of lineage-positive cells in blood, spleen, and bone marrow and LSK cells in bone marrow at week 16 after *in vivo* transduction.

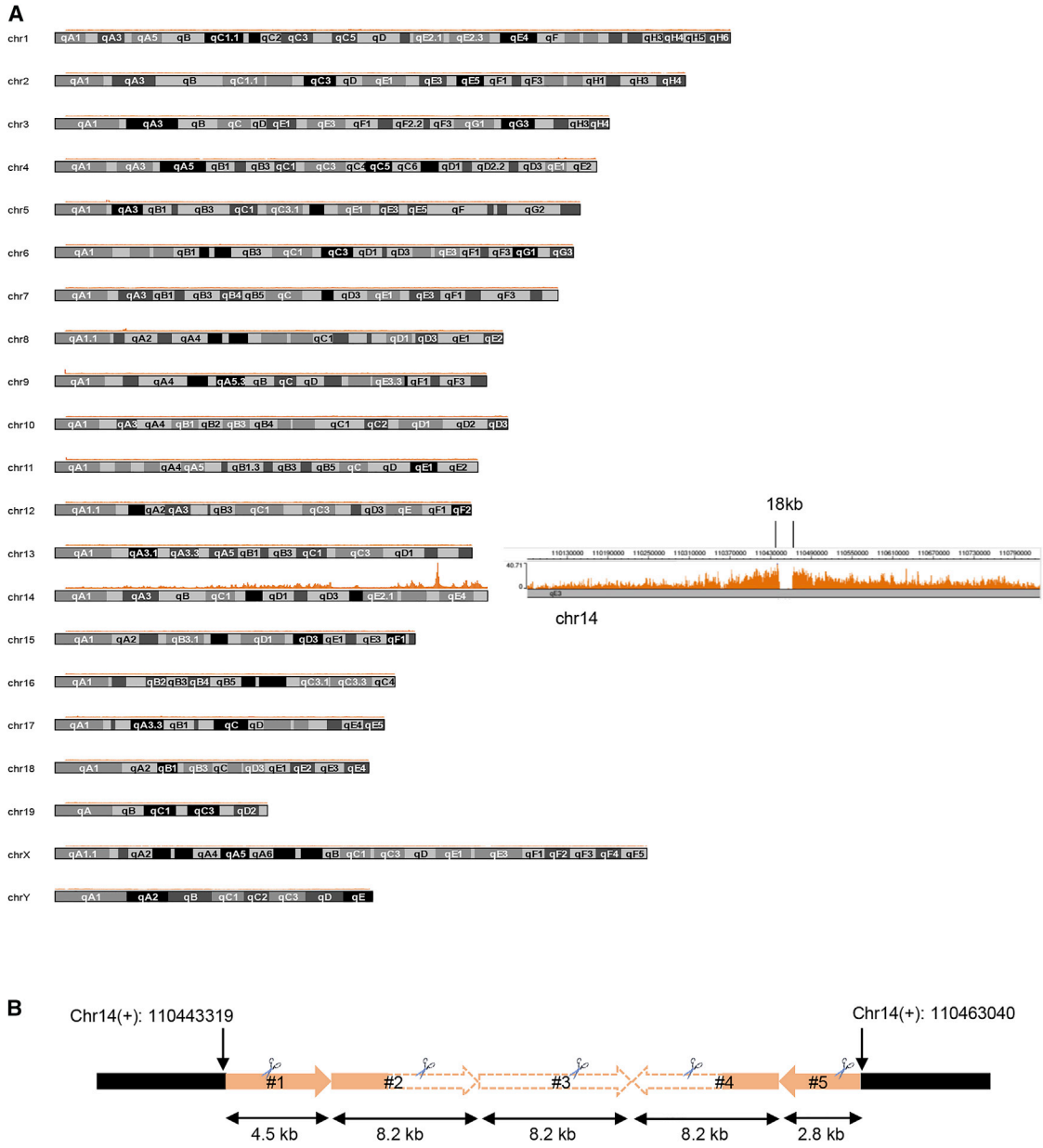

Figure 7. Localization and Structure of the AAVS1 Locus in AAVS1/CD46-tg Mice

(A) TLA data showing mismatches on chromosome 14. The right panel shows an enlarged section of chromosome 14 with the 18-kb gap visible. The gap corresponds to the added human AAVS1 loci. (B) Detailed structure of the AAVS1 loci, indicating the genomic localization. The shaded AAVS1 areas were confirmed by Sanger sequencing. The empty areas were deduced from restriction analysis (see below) and information from The Jackson Laboratory. The CRISPR/Cas9 cleavage sites are indicated by scissors. Repeats 2–4 are complete 8.2-kb human AAVS1 EcoRI fragments, whereas repeats 1 and 5 only contain a fraction of the EcoRI fragment. Notably, repeat 5 lacks a complete 5′ homology arm.

from single cells (Figure 9C). Analysis of colonies from mice with only one band specific for HDR integration into AAVS1 (e.g., mouse 943) showed homogeneous signals in all colonies, whereas colonies from mice with additional off-target integration (e.g. 946) showed a chimeric pattern: nine of ten colonies with only on-target integration and one colony containing both on-target and off-target integrations, which is possible because the average number of integrated transgenes per genome is ~2. Integration site analysis of bone marrow cells in *ex vivo* and *in vivo* transduction studies with HDAd-CRISPR and HDAd-globin-donor vector revealed a similar outcome (Figures 9D and 9E). Off-targeted integration into off-target sites in chr2 or chr5 was also observed (Figures S10 and S11). In the *ex vivo* HSC

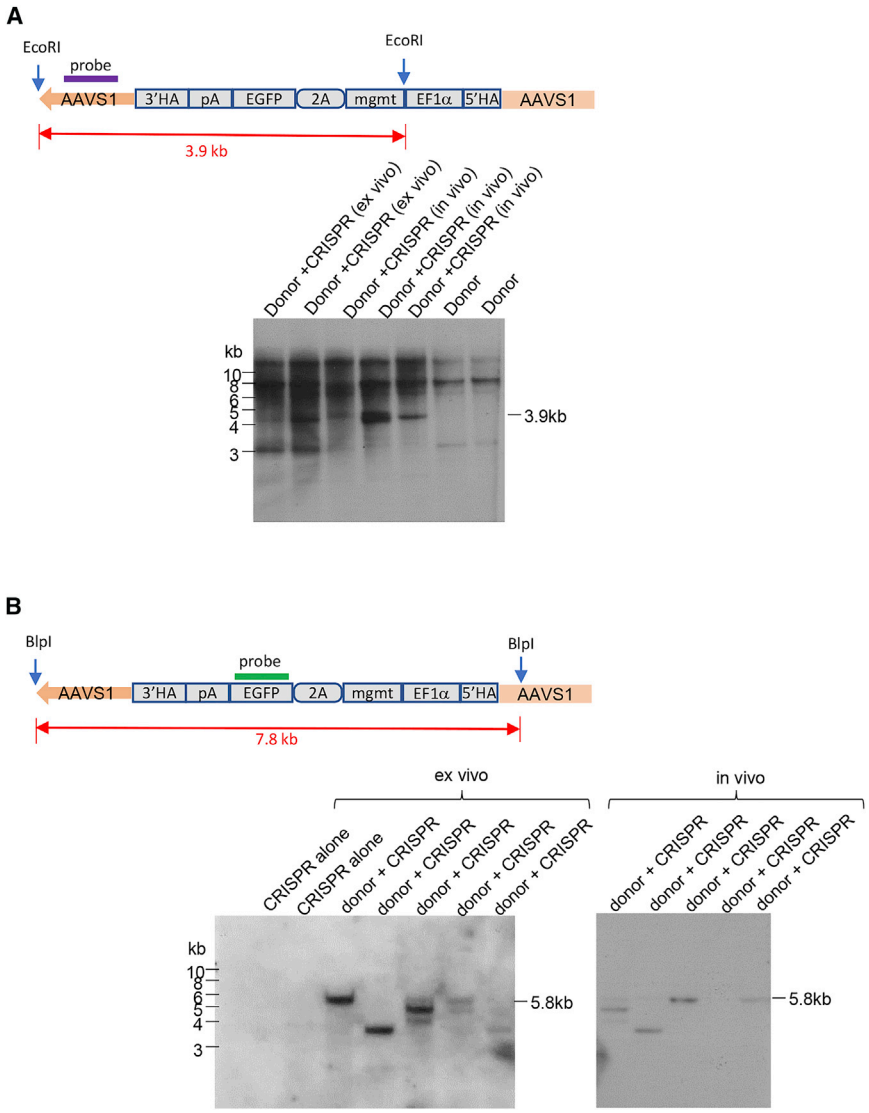

Figure 8. Integration Site Analysis by Southern Blotting of Genomic DNA Isolated at Week 16 after *Ex Vivo* or *In Vivo* HSC Transduction with HDAd-CRISPR + HDAd-GFP-Donor

(A) Hybridization with an AAVS1-specific probe. The top panel shows the expected EcoRI fragment size and the localization of the probe. The bottom panel shows the analysis of individual mice from the *ex vivo* and *in vivo* transduction setting. The larger bands represent non-targeted AAVS1 locus repeats. (B) Hybridization of *BlpI*-digested DNA with a GFP-specific probe. The 7.8-kb predicted band is based on integration into a complete AAVS1 EcoRI fragment. The observed 5.8-kb band resulted from integration into repeat 5, which lacks a complete 5′ homology region. The band pattern is discussed in more detail in the text.

transduction setting with HDAd-CRISPR + HDAd-globin-donor, a higher rate of animals with targeted integrations was found compared with the *in vivo* HSC transduction study with the HDAd-GFP-donor vector. Based on previous reports,[23–25] we speculate that this could be due to higher HDR efficiency based on longer homology regions. A summary of integration site analyses by iPCR can be found in Figure S12.

Overall, our integration studies indicate a high frequency of targeted integrations into AAVS1 loci.

DISCUSSION

Self-inactivating lentivirus vectors, in contrast to gamma-retrovirus vectors, have not been associated with insertion site-associated malignant clonal expansions in clinical HSC gene therapy trials. However, this risk cannot be completely excluded, as indicated by a recent study in non-human primates.[41] Theoretically, the random integration pattern mediated by SB100x transposase and the lack of a preference for integration into activate genes and promoters should be safer, but concerns about genotoxicity remain. Therefore, a major effort in the field is aimed toward targeted transgene integration into preselected sites such as the AAVS1 site. Zinc-finger nuclease mRNA and AAV6-mediated donor template delivery in human HSCs resulted in more than 50% targeted integration into the AAVS1 locus.[17] In other studies that employed an AAVS1-specific CRISPR/Cas9 RNP and AAV6 to deliver the donor template, the frequency of site-specific integration was up to 90%.[19,42] Similar rates were achieved for targeted integration into CCR5.[18]

Our approach for targeted integration into AAVS1 has a number of new aspects. (1) We used a helper-dependent, capsid-modified HDAd5/35++ vector to deliver the donor template. Corresponding vector genomes are double-stranded, linear DNA covalently linked on both ends to the viral TP. It is thought that, in contrast to single-stranded AAV6 donor vectors, double-stranded, linear adenoviral DNA is not an optimal template for HDR. To compensate for this potential disadvantage, we incorporated AAVS1 CRISPR/Cas9 cleavage sites into the HDAd-donor vectors to create free "recombinogenic" DNA ends. (2) Because the insert capacity of HDAd5/35++ vectors is ~30 kb, we were able to incorporate homology arms that would exceed the packaging capacity of rAAV6 or IDLVs. Previous studies suggest that increasing the homology can improve HDR.[23–25]. (3) The large HDAd5/35++ insert capacity also allowed us to include the mgmt^{P140}-based *in vivo* selection cassette into the donor template, mediating selective survival and expansion of progeny cells without affecting the pool of transduced primitive HSCs by short-term treatment with low-dose

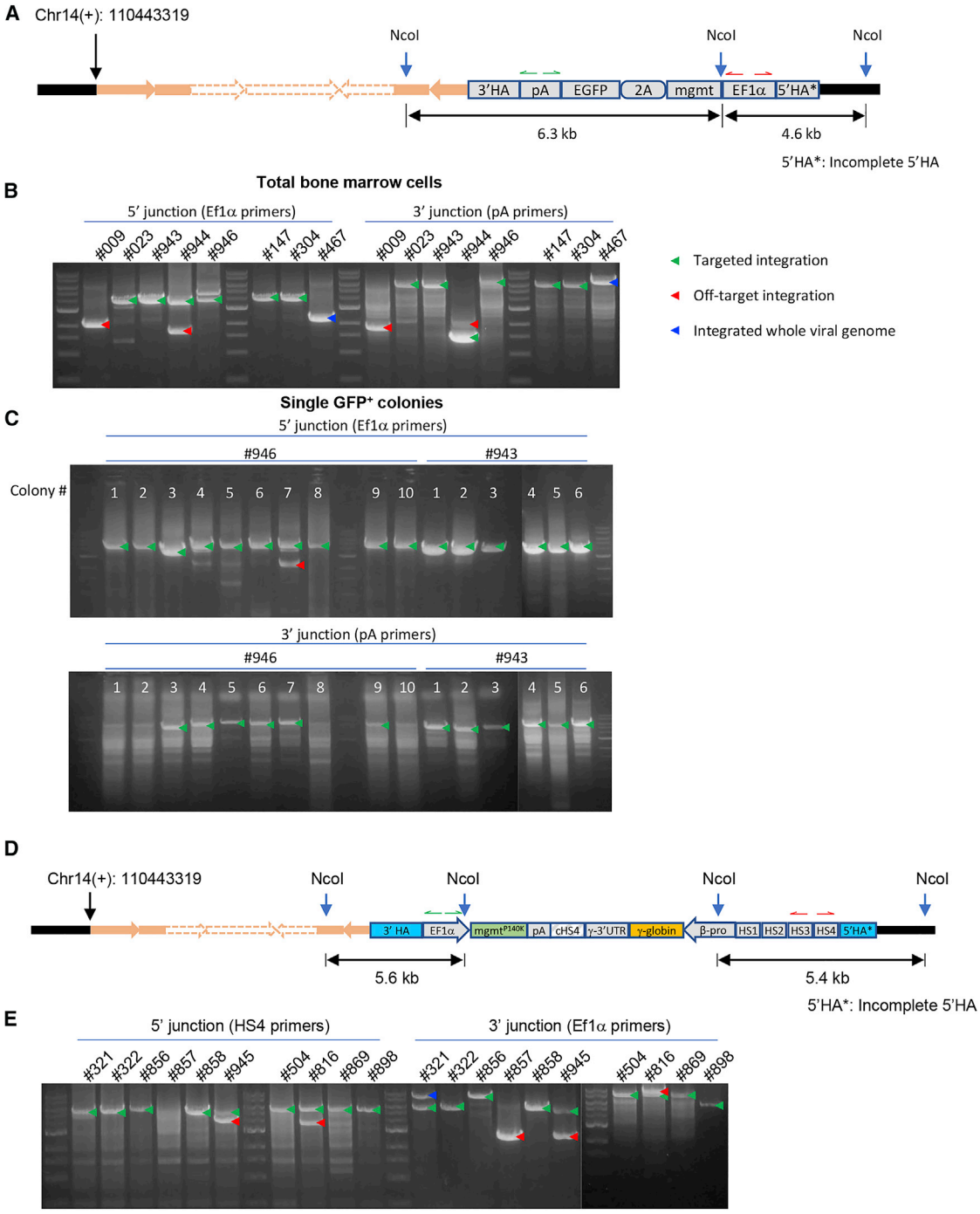

Figure 9. Integration Site Analysis by Inverse PCR (iPCR) of Genomic DNA Isolated at Week 16 after *Ex Vivo* or *In Vivo* HSC Transduction with HDAd-CRISPR + HDAd-GFP-Donor and HDAd-CRISPR + HDAd-γ-Globin-Donor

(A) The locations of *NcoI* sites and primers (half arrows; red, EF1α primers for 5′ junctions; green, pA primers for 3′ junctions). The expected amplicon size at each site for targeted integration in repeat 5 is indicated. (B) iPCR results using genomic DNA from total bone marrow cells. Each lane represents an individual mouse. 009, 023, 943, 944, and 946 are mice after *ex vivo* HSC transduction. 147, 304, and 467 are *in vivo*-transduced animals. (C) iPCR analysis of GFP-positive colonies. Bone marrow Lin^- cells from week 14 mice were plated, and genomic DNA was isolated from GFP-positive colonies 20 days later and used for iPCR. Mice 943 and 946 were analyzed. Each lane

(legend continued on next page)

O^6BG/BCNU.[43] Considering the low efficacy of HDR and, consequently, targeted integration in HSCs,[44] *in vivo* HSC selection appears to be crucial to achieve high transgene marking levels in peripheral blood cells. (4) Finally, because of the ease to produce high yields of HDAd5/35++ vectors and their tropism for primitive HSCs, they can be used for *in vivo* HSC transduction via intravenous injection into mobilized animals. Notably, although CD46 is expressed on all nucleated cells in humans, transgene expression after intravenous injection of HDAd5/35++ vectors was only detected in peripheral blood cells and in a rare subset of splenic cells.[22] This could be due to low CD46 receptor levels and/or poor receptor accessibility in other tissues.

To achieve stable transgene (GFP or γ-globin) expression, coinfection of HDAd-donor and HDAd-CRISPR was essential, suggesting that CRISPR-mediated gDNA breaks and, most likely, the release of the donor template from the HDAd-donor vector greatly stimulated integration. An indicator of transgene integration into HSCs after *in vivo* transduction with HDAd-donor + HDAd-CRISPR was the fraction of mice that displayed stable high-level transgene expression after completion of *in vivo* selection (i.e., responders). It was 6 of 16 (37.5%) for HDAd-GFP-donor + HDAd-CRISPR and 4 of 5 (80%) for HDAd-globin-donor + HDAd-CRISPR. Notably, the responder rate with a high frequency of targeted integration was 100% for both vectors in the *ex vivo* transduction setting. This indicates that a limiting factor for our targeted *in vivo* HSC transduction approach is the efficacy of HSC infection. The initial infection step could theoretically be improved by an optimized HSC mobilization regimen[45] and two rounds of HDAd injection 1 day apart.

Although we did not compare HDAd-donor and AAV6 donor vectors side by side, our data indicate that our vector system is an efficient tool to achieve targeted integrations in HSCs in *ex vivo* and *in vivo* transduction settings. We speculate that key for this is the high efficacy of HDAd-donor vector delivery to the nucleus of non-dividing cells and the HDAd vectors' capacity to incorporate large homology regions.

An important finding in our study was that the targeted integration system conferred higher transgene expression levels than the SB100x-based system in the *in vitro* transduction setting, with the same number of integrated transgene copies per cell (Figures 2C–2F) . Compared with previous studies with the SB100x system done with the same HSC transduction and selection regimen,[28,39] γ-globin levels were also higher after targeted integration (10%–12% γ-globin of mouse β-major globin for SB100x versus 20%–25% γ-globin of mouse β−major globin). Notably, the vector copy number (VCN) in the studies cited above using the SB100x integration system was ~2 copies/cell and comparable with the copy number we found in mice after targeted integration (Figures 5H and 6G).

This is particularly relevant for gene therapy of hemoglobinopathies (β_0/β_0-thalassemia and sickle cell disease), which requires γ-globin at levels that are more than 20% of adult globin levels. In responder mice that were transduced *ex vivo* or *in vivo* with HDAd-CRISPR + HDAd-globin-donor, we achieved these theoretically curative levels. This is an important improvement over our previous study in a thalassemia mouse model, where we used the SB100x transposase system for γ-globin gene addition.[28] We speculate that epigenomic effects on transgene expression are less pronounced after integration into the AAVS1 locus, which is known to maintain an open chromatin configuration in HSCs[2,5,7] and in AAVS1 tg mice.[31] On the other hand, it cannot be excluded that random SB100x-mediated integration places transgenes into regions that are subjected to silencing.

Our integration site analyses suggest a nearly 100% targeted integration efficacy after *in vitro* transduction of HUDEP-2 cells. In *ex vivo* and *in vivo* HSC transduction studies, both Southern blot and iPCR on genomic bone marrow DNA suggested efficient targeted integration in bone marrow HSCs. For example, iPCR of integration junctions documented targeted integration in 75% of mice, with most of these mice having no off-target integration. This was further confirmed by analysis of colonies derived from single CFUs. At a low frequency, integrations were also found in two of the *in silico* predicted CRISPR Cas9 off-target sites. Furthermore, we found full-length HDAd-donor genomes integrated in chr14, the chromosome that carries the AAVS1 loci. We found previously that HDAd ITRs are prone to DNA breaks and that this can result in inefficient integration into genomic sites in which DNA breaks occur.[46,47] Considering recent studies on CRISPR/Cas9-induced undesired large deletions and/or translocations (7–8 kb) around the target site,[48] we speculate that CRISPR-Cas9 DNA breaks far away from the target site could be implicated in the integration of complete HDAd genomes. Overall, reports of large deletions and/or translocations question the safety of CRISPR/Cas9. On the other hand, because no developmental effects associated with CRISPR/Cas9-mediated germline editing in animals have been reported so far, it is likely that cells with such deleterious chromosomal changes are selected out during development. Support for this hypothesis comes from a recent non-human primate (NHP) study in which CRISPR/Cas9-edited HSCs were transplanted, and a 4.9-kb deletion in the HBG1/2 region disappeared in PBMCs over time (O. Humbert et al., 2019, ASGCT, conference). To prove that our HDAd-CRISPR + HDAd-donor *in vivo* HSC transduction approach is safe, similar long-term studies (optimally employing high-accuracy CRISPR/Cas9 versions) in NHPs are required.

From our studies, we also concluded that the AAVS1tg mouse model is suboptimal for targeted integration studies involving

represents one colony. Green arrows, targeted integration; red arrows, off-target integration; blue arrows, integrated whole HDAd viral genome. (D) The diagram shows the locations of *NcoI* sites and primers (half arrows; red, EF1α primers for 5′ junctions; green, pA primers for 3′ junctions). The expected amplicon size at each side for targeted integration in repeat 5 is shown. (E) iPCR results using genomic DNA from total bone marrow cells. Each lane represents one mouse. 321, 322, 856, 857, 858, and 945 are mice after *ex vivo* transduction. 504, 816 869, and 898 are *in vivo*-transduced animals.

CRIRPR/Cas9 because of the presence of multiple AAVS1 target loci, some of which were truncated to a degree where they lost areas of homology with the HDAd-donor vector. The presence of truncated AAVS1 loci also suggests that rearrangement can occur in AAVS1 tg mice, as reported previously.[49] Future studies should be done with a model that contains only mono- or bi-allelic copies of the target site. For example, the human β^s-globin gene or one of the human α-globin genes present in the Townes mouse model for sickle cell disease[50] could be considered as targets, provided that these loci display an open chromatin structure and are accessible to CRISPR/Cas9 in HSCs.

In our studies with AAVS1/CD46-tg mice, we provided proof of targeted integration in HSCs after *ex vivo* or *in vivo* transduction with HDAd-CRISPR + HDAd-donor vector. Although the initial *in vivo* HSC transduction and transgene integration frequency requires improvement, the fact that AAVS1-targeted integration yields higher transgene expression levels and a theoretically safer integration pattern is a critical advantage of our HDAd-based vector system over other currently used approaches.

MATERIALS AND METHODS

Cells

$CD34^+$ cells from G-CSF-mobilized adult donors were provided by Fred Hutch Hematopoietic Cell Procurement and Processing Services. Cells were recovered from frozen stocks and incubated overnight in StemSpan H3000 (STEMCELL Technologies, Vancouver, Canada) with penicillin/streptomycin, Flt3 ligand (Flt3L, 25 ng/mL), interleukin 3 (10 ng/mL), thrombopoietin (TPO; 2 ng/mL), and stem cell factor (SCF; 25 ng/mL). Cells were transduced with HDAd vectors at a MOI of 1,000 or 2,000 vp/cell and analyzed as indicated. HUDEP-2 cells[36] were provided by Ryo Kurita (Central Blood Institute, Japanese Red Cross Society, Department of Research and Development, Tokyo 135-8521, Japan) and Yukio Nakamura (RIKEN BioSource Center, Cell Engineering Division, Ibaraki 305-007, Japan). HUDEP-2 cells were cultured in the presence of SCF, erythropoietin (EPO), doxycycline, and dexamethasone, as described previously.[51] A total of 2×10^5 cells were plated in 24-well ultra-low attachment surface plates (Corning) with 1 mL of medium/well. HDAd vectors at a MOI of 500–1,000 vp/cell were added. The medium was changed 24 h later.

HDAd5/35++ Vectors

HDAd-SB, HDAd-inverted repeat (IR)-GFP/mgmt, and HDAd-IR-γ-globin/mgmt have been described before.[39,43] Details regarding the generation of HDAd-CRISPR, HDAd-GFP-donor, and HDAd-globin-donor are described in the Supplemental Materials and Methods.

For production of HDAd5/35++ vectors, corresponding plasmids were linearized with *PmeI* and rescued in 116 cells[52] with the Ad5/35++-Acr helper vector[20] as described in detail elsewhere.[52] Helper virus contamination levels were found to be <0.05%. Titers were $6–12 \times 10^{12}$ vp/mL.

All HDAd vectors used in this study contain chimeric fibers composed of the Ad5 fiber tail, the Ad35 fiber shaft, and the affinity-enhanced Ad35++ fiber knob.[53]

Mismatch-Sensitive Nuclease T7E1 Assay

gDNA was isolated as described previously.[54] Genomic segments encompassing the AAVS1 target site were amplified by polymerase from *Thermococcus kodakaraensis* (KOD) Hot Start DNA Polymerase (Millipore Sigma, Burlington, MA) using the following primers: AAVS1 forward, 5′-ATCTCACAGGTAAAACTGACGCACGGAG GAACA-3′; reverse, 5′- CGGGTCACCTCTCACTCCTTTCATTT GGGC-3′. PCR products were hybridized and treated with 2.5 units of T7EI (New England Biolabs) for 20 min at 37°C. Digested PCR products were resolved by 6% Tris-borate-EDTA (TBE) PAGE (Bio-Rad) and stained with ethidium bromide. Band intensity was analyzed using ImageJ software. Percent cleavage = (1-sqrt(parental band/(parental band + cleaved bands))) × 100%.

Flow cytometry is described in the Supplemental Materials and Methods.

Lin^- Magnetic-Activated Cell Sorting (MACS) and *Ex Vivo* Transduction

For depletion of lineage-committed cells, a mouse lineage cell depletion kit (Miltenyi Biotec, San Diego, CA) was used according to the manufacturer's instructions. For *ex vivo* transduction, a total of 1×10^7 cells were plated in 10-cm ultra-low attachment surface dishes (Corning Life Sciences) with 7 mL of medium. HDAd vectors were added. Twenty-four hours later, cells were harvested, washed with PBS, and resuspended in PBS at 1×10^6 cells per 200 μL for transplantation.

Real-Time RT-PCR

Total RNA was extracted from 50∼100 μL blood by using TRIzol reagent (Thermo Fisher Scientific) following the manufacture's phenol-chloroform extraction method and then reverse transcribed to generate cDNA using the Quantitect reverse transcription kit from QIAGEN. Potential gDNA contamination was eliminated by treatment of the RNA samples with gDNA wipe-out reagents provided in the kit. Comparative real-time PCR was performed using Power SYBR Green PCR master mix (Applied Biosystems) and run on a StepOnePlus real-time PCR system (Applied Biosystems). The following primer pairs were used: mouse RPL10 (housekeeping) forward 5′-TGAAGA CATGGTTGCTGAGAAG-3′ and reverse 5′-GAACGATTTGGTAG GGTATAGGAG-3′; human γ-globin forward 5′-GGGGCAAGGTGA ATGTGGAAGA-3′ and reverse 5′-CATGATGGCAGAGGCAGAGG AC-3′; mouse β-major globin forward 5′-ATGCCAAAGTGAAG GCCCAT-3′ and reverse 5′-CCCAGCACAATCACGATCAT-3′.

Globin HPLC

Individual globin chain levels were quantified on a Shimadzu Prominence instrument with an SPD-10AV diode array detector and an LC-10AT binary pump (Shimadzu, Kyoto, Japan). A 38%–58% gradient mixture of 0.1% trifluoroacetic acid in water-acetonitrile

was applied at a rate of 1 mL/min using a Vydac C4 reverse-phase column (Hichrom, UK).

CFU Assay

2,500 Lin^- cells were plated in triplicates in ColonyGEL 1202 mouse complete medium (ReachBio, Seattle, WA) and incubated for 12 days at 37°C in 5% CO_2 and maximum humidity. Colonies were enumerated using a Leica MS 5 dissection microscope (Leica Microsystems). For colonies derived from HDAd-GFP-donor-transduced mice, GFP-positive colonies were counted, picked, and analyzed. CFU assays with transduced $CD34^+$ cells were performed using ColonyGEL 1102 human complete medium (ReachBio) according to the manufacturer's protocol. GFP-positive colonies were counted, picked, and analyzed on day 14 after plating.

Measurement of Vector Copy Number

Total DNA from bone marrow cells or single colonies was extracted by PureLink Genomic DNA Mini Kit (Invitrogen). Viral DNA extracted from HDAd-GFP-donor or HDAd-globin-donor was serially diluted and served as a standard curve. qPCR was conducted in duplicate using Power SYBR Green PCR master mix on a StepOnePlus real-time PCR system (Applied Biosystems). 5 ng DNA was used for a 10-μL reaction. The following primer pairs were used: GFP forward 5′- TCGTGACCACCCTGACCTAC-3′ and reverse 5′-GGT CTTGTAGTTGCCGTCGT-3′; mgmt forward 5′-GCTGTCTGGT TGTGAGCAGGGTCT-3′ and reverse 5′-CGGGCTGGTGGAAATA GGCATTC-3′. Human γ-globin primers are described in Real-Time RT-PCR.

Localization of the AAVS1 Locus in AAVS1 tg Mice

TLA libraries were prepared as described previously.[40] Briefly, formaldehyde-crosslinked DNA from total bone marrow cells was digested with *NlaIII*. After ligation and reverse crosslinking, DNA was purified. This product was further digested with *NspI* and ligated to obtain circular chimeric DNA of approximately 2 kb. Chimeric DNA was PCR amplified using AAVS1-specific TLA primers: forward, 5′-GGTTGTCCAGAAAAACGGTGAT-3′; reverse, 5′-CCT CTCACTCCTTTCATTTGGG-3′. TLA libraries from PCR-amplified products were prepared using the Illumina Nextera XT NGS kit according to the manufacturer's protocol. Paired-end sequencing was performed on an Illumina NovaSeq system. The TLA protocol leads to reshuffling of DNA; thus, reads were aligned using Split-Read Aware Aligner BWA[55] using settings bwasw –b 7 as suggested previously (https://github.com/Cergentis/Cergentis_common).[56] The aligned bam files were converted to reads per kilobase of transcript, per million mapped reads (RPKM)-normalized bigwig files using deepTools.[57]. Genome-wide distribution was visualized using the WashU Epigenome Browser.[58]

Southern Blot

gDNA from mouse bone marrow was digested with either EcoRI or *BlpI* and subjected to Southern blotting with either an AAVS1- or GFP-specific probe labeled with ^{32}P using the Prime-It RmT Random Primer labeling kit (Agilent Technologies). Non-incorporated ^{32}P deoxycytidine triphosphate (dCTP) was removed by centrifugation through MicroSpin G25 columns (GE Healthcare). Hybridization was performed in PerfectHyb Plus hybridization buffer (Sigma). Blots were exposed to Amersham Hybond-XL films (GE Healthcare).

Inverse PCR and in and out PCR are described in the Supplemental Materials and Methods.

In Silico Prediction of Off-Target Cleavage Sites

Off-target sites of the AAVS1 guide sequence in the human or mouse genome were predicted using an online tool (https://www.sanger.ac.uk/htgt/wge/find_off_targets_by_seq).

Animal Studies

All experiments involving animals were conducted in accordance with the institutional guidelines set forth by the University of Washington. The University of Washington is accredited by the Association for the Assessment and Accreditation of Laboratory Animal Care International (AALAC), and all live animal work conducted at this university is in accordance with the Office of Laboratory Animal Welfare (OLAW) Public Health Assurance (PHS) policy, United States Department of Agriculture (USDA) Animal Welfare Act and Regulations, the Guide for the Care and Use of Laboratory Animals, and University of Washington's Institutional Animal Care and Use Committee (IACUC) policies. The studies were approved by the University of Washington IACUC (protocol 3108-01). Mice were housed in specific pathogen-free facilities. AAVS1 tg mice (C3;B6-Tg(AAVS1)A1Xob/J) (The Jackson Laboratory) were recovered from cryopreserved embryos of mice developed by Xandra O. Breakefield.[32] Mice were hemizygous for the human AAVS1 locus. AAVS1 tg mice were crossed with human $CD46^{+/+}$ mice to obtain $AAVS1^{+/-}/CD46^{+/-}$ mice for *ex vivo* studies and $AAVS1^{+/-}/CD46^{+/+}$ mice for *in vivo* HSC transduction studies. The following primers were used for genotyping of CD46 mice: forward, 5′-GCCAGTTCATCTTTTGACTCTATTAA-3′; reverse, 5′-AATCA CAGCAATGACCCAAA-3′. Mice homozygous or heterozygous for CD46 were identified by different intensities of CD46 expression on PBMCs, detected by flow cytometry. Genotyping of the AAVS1 transgene was performed by PCR according to The Jackson Laboratory's recommended protocol.

Bone Marrow Lin^- Cell Transplantation

Recipients were female C57BL/6 mice, 6–8 weeks old. On the day of transplantation, recipient mice were irradiated with 1,000 rad. Four hours after irradiation, 1×10^6 Lin^- cells were injected intravenously through the tail vein. This protocol was used for transplantation of *ex vivo*-transduced Lin^- cells and for transplantation into secondary recipients.

HSC Mobilization and *In Vivo* Transduction

This procedure has been described previously.[22] Briefly, HSCs were mobilized in mice by subcutaneous (s.c.) injections of human recombinant G-CSF (5 μg/mouse/day, 4 days) (Amgen, Thousand Oaks, CA), followed by an s.c. injection of AMD3100 (5 mg/kg)

(Sigma-Aldrich) on day 5. In addition, animals received dexamethasone (10 mg/kg) intraperitoneally (i.p.) 16 h and 2 h before virus injection. Thirty and 60 min after AMD3100, animals were injected intravenously with HDAd-CRISPR and HDAd-GFP-donor or HDAd-globin-donor through the retro-orbital plexus with a dose of 4×10^{10} vp for each virus per injection. Four weeks later, mice were injected with O6-BG (15 mg/kg, i.p.) twice, 30 min apart. One hour after the second injection of O6-BG, mice were injected with BCNU (5 mg/kg, i.p.). The BCNU dose was increased to 7.5 and 10 mg/kg in the second and third cycle, respectively. Both BCNU and O6-BG were from Sigma-Aldrich.

Statistical Analyses

For comparisons of multiple groups, one-way and two-way ANOVA with Bonferroni post-testing for multiple comparisons was employed. Statistical analysis was performed using GraphPad Prism version 6.01 (GraphPad, La Jolla, CA).

SUPPLEMENTAL INFORMATION

Supplemental Information can be found online at https://doi.org/10.1016/j.ymthe.2019.08.006.

AUTHOR CONTRIBUTIONS

A.L. provided the conceptual framework for the study. C.L. and A.L. designed the experiments. C.L., A.S.M., S.G., M.W., and A.G. performed the experiments. T.P. and R.D.H. provided critical comments on the manuscript. A.L. wrote the manuscript.

CONFLICTS OF INTEREST

The authors declare no competing interests.

ACKNOWLEDGMENTS

We thank Nikoletta Psatha for helpful advice and technical help. We thank Pavel Sova for support with next-generation sequencing. The study was supported by grants R21CA193077, R01HL128288, and R01HL141781; a grant from the Bill and Melinda Gates Foundation (to A.L.); and grant R01 DK 101328 (to T.P.).

REFERENCES

1. Naldini, L. (2019). Genetic engineering of hematopoiesis: current stage of clinical translation and future perspectives. EMBO Mol. Med. *11*, e9958.
2. Wang, G.P., Ciuffi, A., Leipzig, J., Berry, C.C., and Bushman, F.D. (2007). HIV integration site selection: analysis by massively parallel pyrosequencing reveals association with epigenetic modifications. Genome Res. *17*, 1186–1194.
3. Papapetrou, E.P., Lee, G., Malani, N., Setty, M., Riviere, I., Tirunagari, L.M., Kadota, K., Roth, S.L., Giardina, P., Viale, A., et al. (2011). Genomic safe harbors permit high β-globin transgene expression in thalassemia induced pluripotent stem cells. Nat. Biotechnol. *29*, 73–78.
4. Muzyczka, N. (1992). Use of adeno-associated virus as a general transduction vector for mammalian cells. Curr. Top. Microbiol. Immunol. *158*, 97–129.
5. Hüser, D., Gogol-Döring, A., Lutter, T., Weger, S., Winter, K., Hammer, E.M., Cathomen, T., Reinert, K., and Heilbronn, R. (2010). Integration preferences of wild-type AAV-2 for consensus rep-binding sites at numerous loci in the human genome. PLoS Pathog. *6*, e1000985.
6. Henckaerts, E., and Linden, R.M. (2010). Adeno-associated virus: a key to the human genome? Future Virol. *5*, 555–574.
7. van Rensburg, R., Beyer, I., Yao, X.Y., Wang, H., Denisenko, O., Li, Z.Y., Russell, D.W., Miller, D.G., Gregory, P., Holmes, M., et al. (2013). Chromatin structure of two genomic sites for targeted transgene integration in induced pluripotent stem cells and hematopoietic stem cells. Gene Ther. *20*, 201–214.
8. Lombardo, A., Cesana, D., Genovese, P., Di Stefano, B., Provasi, E., Colombo, D.F., Neri, M., Magnani, Z., Cantore, A., Lo Riso, P., et al. (2011). Site-specific integration and tailoring of cassette design for sustainable gene transfer. Nat. Methods *8*, 861–869.
9. Ogata, T., Kozuka, T., and Kanda, T. (2003). Identification of an insulator in AAVS1, a preferred region for integration of adeno-associated virus DNA. J. Virol. *77*, 9000–9007.
10. Voigt, K., Izsvák, Z., and Ivics, Z. (2008). Targeted gene insertion for molecular medicine. J. Mol. Med. (Berl.) *86*, 1205–1219.
11. Lombardo, A., and Naldini, L. (2014). Genome editing: a tool for research and therapy: targeted genome editing hits the clinic. Nat. Med. *20*, 1101–1103.
12. Blair, J.D., Bateup, H.S., and Hockemeyer, D.F. (2016). Establishment of Genome-edited Human Pluripotent Stem Cell Lines: From Targeting to Isolation. J. Vis. Exp. *108*, e53583.
13. Dreyer, A.K., Hoffmann, D., Lachmann, N., Ackermann, M., Steinemann, D., Timm, B., Siler, U., Reichenbach, J., Grez, M., Moritz, T., et al. (2015). TALEN-mediated functional correction of X-linked chronic granulomatous disease in patient-derived induced pluripotent stem cells. Biomaterials *69*, 191–200.
14. Kuhn, A., Ackermann, M., Mussolino, C., Cathomen, T., Lachmann, N., and Moritz, T. (2017). TALEN-mediated functional correction of human iPSC-derived macrophages in context of hereditary pulmonary alveolar proteinosis. Sci. Rep. *7*, 15195.
15. Li, S.J., Luo, Y., Zhang, L.M., Yang, W., and Zhang, G.G. (2017). Targeted introduction and effective expression of hFIX at the AAVS1 locus in mesenchymal stem cells. Mol. Med. Rep. *15*, 1313–1318.
16. Rio, P., Baños, R., Lombardo, A., Quintana-Bustamante, O., Alvarez, L., Garate, Z., Genovese, P., Almarza, E., Valeri, A., Díez, B., et al. (2014). Targeted gene therapy and cell reprogramming in Fanconi anemia. EMBO Mol. Med. *6*, 835–848.
17. De Ravin, S.S., Reik, A., Liu, P.Q., Li, L., Wu, X., Su, L., Raley, C., Theobald, N., Choi, U., Song, A.H., et al. (2016). Targeted gene addition in human CD34(+) hematopoietic cells for correction of X-linked chronic granulomatous disease. Nat. Biotechnol. *34*, 424–429.
18. Hung, K.L., Meitlis, I., Hale, M., Chen, C.Y., Singh, S., Jackson, S.W., Miao, C.H., Khan, I.F., Rawlings, D.J., and James, R.G. (2018). Engineering Protein-Secreting Plasma Cells by Homology-Directed Repair in Primary Human B Cells. Mol. Ther. *26*, 456–467.
19. Johnson, M.J., Laoharawee, K., Lahr, W.S., Webber, B.R., and Moriarity, B.S. (2018). Engineering of Primary Human B cells with CRISPR/Cas9 Targeted Nuclease. Sci. Rep. *8*, 12144.
20. Li, C., Psatha, N., Sova, P., Gil, S., Wang, H., Kim, J., Kulkarni, C., Valensisi, C., Hawkins, R.D., Stamatoyannopoulos, G., and Lieber, A. (2018). Reactivation of γ-globin in adult β-YAC mice after ex vivo and in vivo hematopoietic stem cell genome editing. Blood *131*, 2915–2928.
21. Saydaminova, K., Ye, X., Wang, H., Richter, M., Ho, M., Chen, H., Xu, N., Kim, J.S., Papapetrou, E., Holmes, M.C., et al. (2015). Efficient genome editing in hematopoietic stem cells with helper-dependent Ad5/35 vectors expressing site-specific endonucleases under microRNA regulation. Mol. Ther. Methods Clin. Dev. *1*, 14057.
22. Richter, M., Saydaminova, K., Yumul, R., Krishnan, R., Liu, J., Nagy, E.E., Singh, M., Izsvák, Z., Cattaneo, R., Uckert, W., et al. (2016). In vivo transduction of primitive mobilized hematopoietic stem cells after intravenous injection of integrating adenovirus vectors. Blood *128*, 2206–2217.
23. Balamotis, M.A., Huang, K., and Mitani, K. (2004). Efficient delivery and stable gene expression in a hematopoietic cell line using a chimeric serotype 35 fiber pseudotyped helper-dependent adenoviral vector. Virology *324*, 229–237.
24. Ohbayashi, F., Balamotis, M.A., Kishimoto, A., Aizawa, E., Diaz, A., Hasty, P., Graham, F.L., Caskey, C.T., and Mitani, K. (2005). Correction of chromosomal mutation and random integration in embryonic stem cells with helper-dependent adenoviral vectors. Proc. Natl. Acad. Sci. USA *102*, 13628–13633.

25. Suzuki, K., Mitsui, K., Aizawa, E., Hasegawa, K., Kawase, E., Yamagishi, T., Shimizu, Y., Suemori, H., Nakatsuji, N., and Mitani, K. (2008). Highly efficient transient gene expression and gene targeting in primate embryonic stem cells with helper-dependent adenoviral vectors. Proc. Natl. Acad. Sci. USA *105*, 13781–13786.

26. Chu, V.T., Weber, T., Wefers, B., Wurst, W., Sander, S., Rajewsky, K., and Kühn, R. (2015). Increasing the efficiency of homology-directed repair for CRISPR-Cas9-induced precise gene editing in mammalian cells. Nat. Biotechnol. *33*, 543–548.

27. Li, K., Wang, G., Andersen, T., Zhou, P., and Pu, W.T. (2014). Optimization of genome engineering approaches with the CRISPR/Cas9 system. PLoS ONE *9*, e105779.

28. Wang, H., Georgakopoulou, A., Psatha, N., Li, C., Capsali, C., Samal, H.B., Anagnostopoulos, A., Ehrhardt, A., Izsvák, Z., Papayannopoulou, T., et al. (2019). In vivo hematopoietic stem cell gene therapy ameliorates murine thalassemia intermedia. J. Clin. Invest. *129*, 598–615.

29. Samulski, R.J., Zhu, X., Xiao, X., Brook, J.D., Housman, D.E., Epstein, N., and Hunter, L.A. (1991). Targeted integration of adeno-associated virus (AAV) into human chromosome 19. EMBO J. *10*, 3941–3950.

30. Rizzuto, G., Gorgoni, B., Cappelletti, M., Lazzaro, D., Gloaguen, I., Poli, V., Sgura, A., Cimini, D., Ciliberto, G., Cortese, R., et al. (1999). Development of animal models for adeno-associated virus site-specific integration. J. Virol. *73*, 2517–2526.

31. Young, S.M., Jr., McCarty, D.M., Degtyareva, N., and Samulski, R.J. (2000). Roles of adeno-associated virus Rep protein and human chromosome 19 in site-specific recombination. J. Virol. *74*, 3953–3966.

32. Bakowska, J.C., Di Maria, M.V., Camp, S.M., Wang, Y., Allen, P.D., and Breakefield, X.O. (2003). Targeted transgene integration into transgenic mouse fibroblasts carrying the full-length human AAVS1 locus mediated by HSV/AAV rep(+) hybrid amplicon vector. Gene Ther. *10*, 1691–1702.

33. Kemper, C., Leung, M., Stephensen, C.B., Pinkert, C.A., Liszewski, M.K., Cattaneo, R., and Atkinson, J.P. (2001). Membrane cofactor protein (MCP; CD46) expression in transgenic mice. Clin. Exp. Immunol. *124*, 180–189.

34. Shenk, T. (1996). Adenoviridae. In Fields Virology, D.M. Knipe and P.M. Howley, eds. (Lippincott-Raven), pp. 2111–2148.

35. Cristea, S., Freyvert, Y., Santiago, Y., Holmes, M.C., Urnov, F.D., Gregory, P.D., and Cost, G.J. (2013). In vivo cleavage of transgene donors promotes nuclease-mediated targeted integration. Biotechnol. Bioeng. *110*, 871–880.

36. Kurita, R., Suda, N., Sudo, K., Miharada, K., Hiroyama, T., Miyoshi, H., Tani, K., and Nakamura, Y. (2013). Establishment of immortalized human erythroid progenitor cell lines able to produce enucleated red blood cells. PLoS ONE *8*, e59890.

37. Boehme, P., Zhang, W., Solanki, M., Ehrke-Schulz, E., and Ehrhardt, A. (2016). A High-Capacity Adenoviral Hybrid Vector System Utilizing the Hyperactive Sleeping Beauty Transposase SB100X for Enhanced Integration. Mol. Ther. Nucleic Acids *5*, e337.

38. Li, C., Psatha, N., Gil, S., Wang, H., Papayannopoulou, T., and Lieber, A. (2018). HDAd5/35^{++} Adenovirus Vector Expressing Anti-CRISPR Peptides Decreases CRISPR/Cas9 Toxicity in Human Hematopoietic Stem Cells. Mol. Ther. Methods Clin. Dev. *9*, 390–401.

39. Li, C., Psatha, N., Wang, H., Singh, M., Samal, H.B., Zhang, W., Ehrhardt, A., Izsvák, Z., Papayannopoulou, T., and Lieber, A. (2018). Integrating HDAd5/35++ Vectors as a New Platform for HSC Gene Therapy of Hemoglobinopathies. Mol. Ther. Methods Clin. Dev. *9*, 142–152.

40. de Vree, P.J., de Wit, E., Yilmaz, M., van de Heijning, M., Klous, P., Verstegen, M.J., Wan, Y., Teunissen, H., Krijger, P.H., Geeven, G., et al. (2014). Targeted sequencing by proximity ligation for comprehensive variant detection and local haplotyping. Nat. Biotechnol. *32*, 1019–1025.

41. Espinoza, D.A., Fan, X., Yang, D., Cordes, S.F., Truitt, L.L., Calvo, K.R., Yabe, I.M., Demirci, S., Hope, K.J., Hong, S.G., et al. (2019). Aberrant Clonal Hematopoiesis following Lentiviral Vector Transduction of HSPCs in a Rhesus Macaque. Mol. Ther. *27*, 1074–1086.

42. Martin, R.M., Ikeda, K., Cromer, M.K., Uchida, N., Nishimura, T., Romano, R., Tong, A.J., Lemgart, V.T., Camarena, J., Pavel-Dinu, M., et al. (2019). Highly Efficient and Marker-free Genome Editing of Human Pluripotent Stem Cells by CRISPR-Cas9 RNP and AAV6 Donor-Mediated Homologous Recombination. Cell Stem Cell *24*, 821–828.5.

43. Wang, H., Richter, M., Psatha, N., Li, C., Kim, J., Liu, J., Ehrhardt, A., Nilsson, S.K., Cao, B., Palmer, D., et al. (2017). A Combined *In Vivo* HSC Transduction/Selection Approach Results in Efficient and Stable Gene Expression in Peripheral Blood Cells in Mice. Mol. Ther. Methods Clin. Dev. *8*, 52–64.

44. Genovese, P., Schiroli, G., Escobar, G., Tomaso, T.D., Firrito, C., Calabria, A., Moi, D., Mazzieri, R., Bonini, C., Holmes, M.C., et al. (2014). Targeted genome editing in human repopulating haematopoietic stem cells. Nature *510*, 235–240.

45. Psatha, N., Sgouramali, E., Gkountis, A., Siametis, A., Baliakas, P., Constantinou, V., Athanasiou, E., Arsenakis, M., Anagnostopoulos, A., Papayannopoulou, T., et al. (2014). Superior long-term repopulating capacity of G-CSF+plerixafor-mobilized blood: implications for stem cell gene therapy by studies in the Hbb(th-3) mouse model. Hum. Gene Ther. Methods *25*, 317–327.

46. Wang, H., Shayakhmetov, D.M., Leege, T., Harkey, M., Li, Q., Papayannopoulou, T., Stamatoyannopolous, G., and Lieber, A. (2005). A capsid-modified helper-dependent adenovirus vector containing the beta-globin locus control region displays a nonrandom integration pattern and allows stable, erythroid-specific gene expression. J. Virol. *79*, 10999–11013.

47. Wang, H., and Lieber, A. (2006). A helper-dependent capsid-modified adenovirus vector expressing adeno-associated virus rep78 mediates site-specific integration of a 27-kilobase transgene cassette. J. Virol. *80*, 11699–11709.

48. Kosicki, M., Tomberg, K., and Bradley, A. (2018). Repair of double-strand breaks induced by CRISPR-Cas9 leads to large deletions and complex rearrangements. Nat. Biotechnol. *36*, 765–771.

49. Linden, R.M., Winocour, E., and Berns, K.I. (1996). The recombination signals for adeno-associated virus site-specific integration. Proc. Natl. Acad. Sci. USA *93*, 7966–7972.

50. Wu, L.C., Sun, C.W., Ryan, T.M., Pawlik, K.M., Ren, J., and Townes, T.M. (2006). Correction of sickle cell disease by homologous recombination in embryonic stem cells. Blood *108*, 1183–1188.

51. Canver, M.C., Smith, E.C., Sher, F., Pinello, L., Sanjana, N.E., Shalem, O., Chen, D.D., Schupp, P.G., Vinjamur, D.S., Garcia, S.P., et al. (2015). BCL11A enhancer dissection by Cas9-mediated in situ saturating mutagenesis. Nature *527*, 192–197.

52. Palmer, D., and Ng, P. (2003). Improved system for helper-dependent adenoviral vector production. Mol. Ther. *8*, 846–852.

53. Wang, H., Liu, Y., Li, Z., Tuve, S., Stone, D., Kalyushniy, O., Shayakhmetov, D., Verlinde, C.L., Stehle, T., McVey, J., et al. (2008). In vitro and in vivo properties of adenovirus vectors with increased affinity to CD46. J. Virol. *82*, 10567–10579.

54. Miller, J.C., Holmes, M.C., Wang, J., Guschin, D.Y., Lee, Y.L., Rupniewski, I., Beausejour, C.M., Waite, A.J., Wang, N.S., Kim, K.A., et al. (2007). An improved zinc-finger nuclease architecture for highly specific genome editing. Nat. Biotechnol. *25*, 778–785.

55. Li, H., and Durbin, R. (2010). Fast and accurate long-read alignment with Burrows-Wheeler transform. Bioinformatics *26*, 589–595.

56. Cain-Hom, C., Splinter, E., van Min, M., Simonis, M., van de Heijning, M., Martinez, M., Asghari, V., Cox, J.C., and Warming, S. (2017). Efficient mapping of transgene integration sites and local structural changes in Cre transgenic mice using targeted locus amplification. Nucleic Acids Res. *45*, e62.

57. Ramírez, F., Dündar, F., Diehl, S., Grüning, B.A., and Manke, T. (2014). deepTools: a flexible platform for exploring deep-sequencing data. Nucleic Acids Res. *42*, W187-91.

58. Zhou, X., Maricque, B., Xie, M., Li, D., Sundaram, V., Martin, E.A., Koebbe, B.C., Nielsen, C., Hirst, M., Farnham, P., et al. (2011). The Human Epigenome Browser at Washington University. Nat. Methods *8*, 989–990.

59. Lisowski, L., and Sadelain, M. (2007). Locus control region elements HS1 and HS4 enhance the therapeutic efficacy of globin gene transfer in beta-thalassemic mice. Blood *110*, 4175–4178.

60. Emery, D.W., Yannaki, E., Tubb, J., and Stamatoyannopoulos, G. (2000). A chromatin insulator protects retrovirus vectors from chromosomal position effects. Proc. Natl. Acad. Sci. USA *97*, 9150–9155.

YMTHE, Volume *27*

Supplemental Information

Targeted Integration and High-Level Transgene Expression in AAVS1 Transgenic Mice after *In Vivo* HSC Transduction with HDAd5/35++ Vectors

Chang Li, Arpit Suresh Mishra, Sucheol Gil, Meng Wang, Aphrodite Georgakopoulou, Thalia Papayannopoulou, R. David Hawkins, and André Lieber

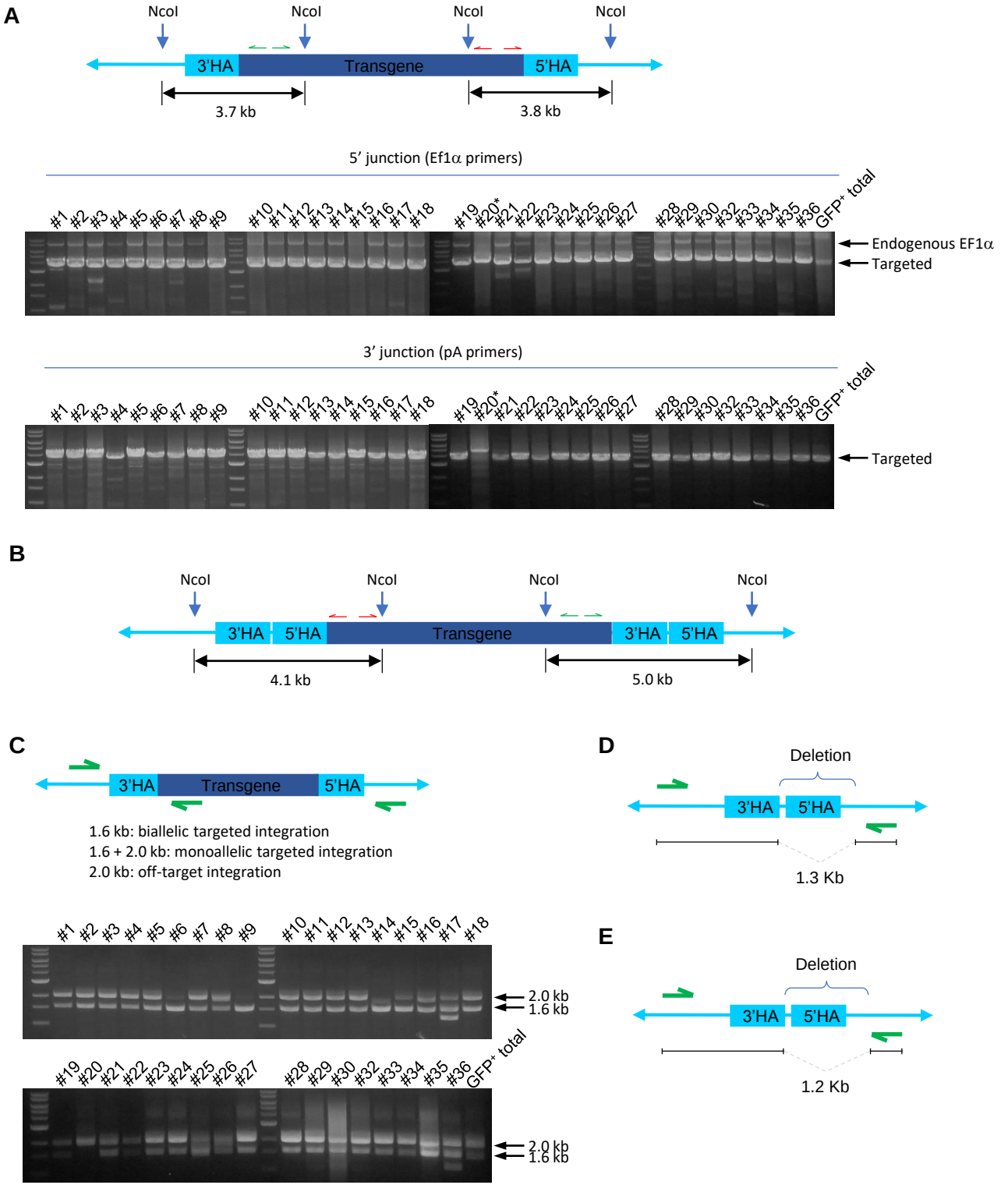
A
NcoI
NcoI
NcoI
NcoI
3'HA
Transgene
5'HA
3.7 kb
3.8 kb
5' junction (Ef1α primers)
#1 #2 #3 #4 #5 #6 #7 #8 #9 #10 #11 #12 #13 #14 #15 #16 #17 #18 #19 #20* #21 #22 #23 #24 #25 #26 #27 #28 #29 #30 #32 #33 #34 #35 #36 GFP+ total
Endogenous EF1α
Targeted
3' junction (pA primers)
#1 #2 #3 #4 #5 #6 #7 #8 #9 #10 #11 #12 #13 #14 #15 #16 #17 #18 #19 #20* #21 #22 #23 #24 #25 #26 #27 #28 #29 #30 #32 #33 #34 #35 #36 GFP+ total
Targeted
B
NcoI
NcoI
NcoI
NcoI
3'HA
5'HA
Transgene
3'HA
5'HA
4.1 kb
5.0 kb
C
3'HA
Transgene
5'HA
1.6 kb: biallelic targeted integration
1.6 + 2.0 kb: monoallelic targeted integration
2.0 kb: off-target integration
#1 #2 #3 #4 #5 #6 #7 #8 #9 #10 #11 #12 #13 #14 #15 #16 #17 #18
2.0 kb
1.6 kb
#19 #20 #21 #22 #23 #24 #25 #26 #27 #28 #29 #30 #32 #33 #34 #35 #36 GFP+ total
2.0 kb
1.6 kb
D
Deletion
3'HA
5'HA
1.3 Kb
E
Deletion
3'HA
5'HA
1.2 Kb

Supplementary Figure S1. Integration analysis of HUDEP-2 clones transduced with vectors for targeted integration. A) Integration site analysis by inverse PCR. The upper diagram shows the locations of *NcoI* sites and primers (half arrows. Red: EF1α primers for 5'- junctions; green: pA primers for 3' junctions). HA: homology arms. The expected amplicon size at each side for targeted integration is indicated. The lower gel pictures show iPCR results. Each lane represents one cell clone. An extra band derived from the endogenous EF1α promoter was detected. For clone #20, although the amplicon size is different from prediction, cloning and sequencing revealed that it is a clone with targeted integration. **B)** Diagram showing the integration pattern in clone #20. **C)** In-/out-PCR analysis. The upper diagram shows the location of primers. Expected product sizes for various integration patterns are listed. The lower gel pictures demonstrate that most clones had monoallelic targeted integration. **D-E)** Diagram explaining the origin of the smaller bands in #17 and #36 in C), respectively. Both smaller bands resulted from large fragment deletions.

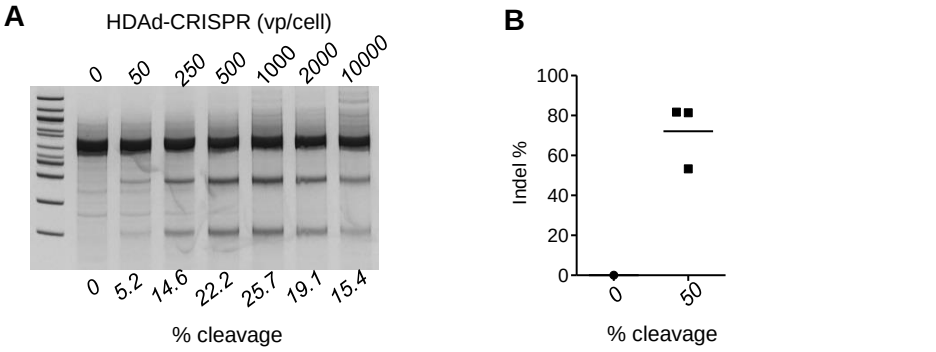

C

			# of reads	% of reads
	TGTCCCCTCCACCCCACAGTGGGGCCACTAGGGACAGGATTGGTGACAGAAAAGCCCCATCCTTAGGCCTCCTCCTTCCT	0	19505	15.8%
1	TGTCCCCTCCACCCCACAGTGGGGCC-------ACAGGATTGGTGACAGAAAAGCCCCATCCTTAGGCCTCCTCCTTCCT	-7	348	0.3%
2	TGTCCCCTCCACCCCACAGTGGGGCCACTAGGGACA-----GGTGACAGAAAAGCCCCATCCTTAGGCCTCCTCCTTCCT	-5	10016	7.5%
3	TGTCCCCTCCACCCCACAGTGGGGCCACTAGGGACA-----GGTGACAGAAAATCCCCATCCTTAGGCCTCCTCCTTCCT	-5	899	0.7%
4	TGTCCCCTCCACCCCACAGTGGGGCCACTAG-----GGATTGGTGACAGAAAAGCCCCATCCTTAGGCCTCCTCCTTCCT	-5	703	0.5%
5	TGTCCCCTCCACCCCACAGTGGGGCCACTAGGGACA-----GGTGACAGAAAAGCCCCATCCTTAGGCCTCCTCCTTCCT	-5	699	0.5%
6	TGTCCCCTCCACCCCACAGTGGGGCCACTAGGGACA-----GGTGACAGAAAAGCCCCATCCTTAGGCCTCCTCCTTCCT	-5	300	0.2%
7	TGTCCCCTCCACCCCACAGTGGGGCCACTAGG----GGATTGGTGACAGAAAAGCCCCATCCTTAGGCCTCCTCCTTCCT	-4	418	0.3%
8	TGTCCCCTCCACCCCACAGTGGGGCCACTAGG---AGGATTGGTGACAGAAAAGCCCCATCCTTAGGCCTCCTCCTTCCT	-3	13995	10.5%
9	TGTCCCCTCCACCCCACAGTGGGGCCACTAG---CAGGATTGGTGACAGAAAAGCCCCATCCTTAGGCCTCCTCCTTCCT	-3	10311	7.7%
10	TGTCCCCTCCACCCCACAGTGGGGCCACTAGG---CGGATTGGTGACAGAAAAGCCCCATCCTTAGGCCTCCTCCTTCCT	-3	1586	1.2%
11	TGTCCCCTCCACCCCACAGTGGGGCCACTAG---CCGGATTGGTGACAGAAAAGCCCCATCCTTAGGCCTCCTCCTTCCT	-3	1113	0.8%
12	TGTCCCCTCCACCCCACAGTGGGGCCACTAGG---AGGATTGGTGACAGAAAAGCCCCATCCTTAGGCCTCCTCCTTCCT	-3	713	0.5%
13	TGTCCCCTCCACCCCACAGTGGGGCCACTAGG---AGTATTGGTGACAGAAAAGCCCCATCCTTAGGCCTCCTCCTTCCT	-3	524	0.4%
14	TGTCCCCTCCACCCCACAGTGGGGCCACTAG---CAGGATTGGTGACAGAAAAGCCCCATCCTTAGGCCTCCTCCTTCCT	-3	503	0.4%
15	TGTCCCCTCCACCCCACAGTGGGGCCACTAGG---AGGATTGGTGACAGAACAGCCCCATCCTTAGGCCTCCTCCTTCCT	-3	361	0.3%
16	TGTCCCCTCCACCCCACAGTGGGGCCACTAG---CAGTATTGGTGACAGAAAAGCCCCATCCTTAGGCCTCCTCCTTCCT	-3	335	0.3%
17	TGTCCCCTCCACCCCACAGTGGGGCCACTAG---CAGGATTGGTGACAGAACAGCCCCATCCTTAGGCCTCCTCCTTCCT	-3	290	0.2%
18	TGTCCCCTCCACCCCACAGTGGGGCCACTAGGGAC--GATTGGTGACAGAAAAGCCCCATCCTTAGGCCTCCTCCTTCCT	-2	17441	13.1%
19	TGTCCCCTCCACCCCACAGTGGGGCCACTAGGG--AGGATTGGTGACAGAAAAGCCCCATCCTTAGGCCTCCTCCTTCCT	-2	16863	12.7%
20	TGTCCCCTCCACCCCACAGTGGGGCCACTAGG--CAGGATTGGTGACAGAAAAGCCCCATCCTTAGGCCTCCTCCTTCCT	-2	6392	4.8%
21	TGTCCCCTCCACCCCACAGTGGGGCCACTAGGG--ATGATTGGTGACAGAAAAGCCCCATCCTTAGGCCTCCTCCTTCCT	-2	600	0.5%
22	TGTCCCCTCCACCCCACAGTGGGGCCACTAGGGAC--GCTTGGTGACAGAAAAGCCCCATCCTTAGGCCTCCTCCTTCCT	-2	566	0.4%
23	TGTCCCCTCCACCCCACAGTGGGGCCACTAGGG--AGGCTTGGTGACAGAAAAGCCCCATCCTTAGGCCTCCTCCTTCCT	-2	559	0.4%
24	TGTCCCCTCCACCCCACAGTGGGGCCACTAGGGAC--GATTGGTGACAGACAAGCCCCATCCTTAGGCCTCCTCCTTCCT	-2	452	0.3%
25	TGTCCCCTCCACCCCACAGTGGGGCCACTAGGG--AGGATTGGTGACAGACAAGCCCCATCCTTAGGCCTCCTCCTTCCT	-2	445	0.3%
26	TGTCCCCTCCACCCCACAGTGGGGCCACTAGGGAC--GATTGGTGCCAGAAAAGCCCCATCCTTAGGCCTCCTCCTTCCT	-2	378	0.3%
27	TGTCCCCTCCACCCCACAGTGGGGCCACTAGGG--AGGATTGGTGCCAGAAAAGCCCCATCCTTAGGCCTCCTCCTTCCT	-2	318	0.2%
28	TGTCCCCTCCACCCCACAGTGGGGCCACTAGGGACA-GATTGGTGACAGAAAAGCCCCATCCTTAGGCCTCCTCCTTCCT	-1	544	0.4%

Supplementary Figure S2. Cleavage of AAVS1 target site in AAVS1/CD46tg mice. A) *In vitro* analysis. Target site cleavage frequency in bone marrow lineage-negative cells from AAVS1/CD46tg mice measured three days after HDAd-CRISPR transduction at the indicated MOIs. **B)** Percentage of total AAVS1 indels obtained by deep sequencing of DNA from total bone marrow mononuclear cells at week 16 after transplantation (see Fig.3A). Each symbol is an individual animal. **C)** Top 30 most frequent indels found in a mouse. Representative data are shown. The yellow sequence shows the target of the guide RNA with the PAM sequence marked in blue. The CRISPR/Cas9 cleavage site is marked by a vertical arrow.

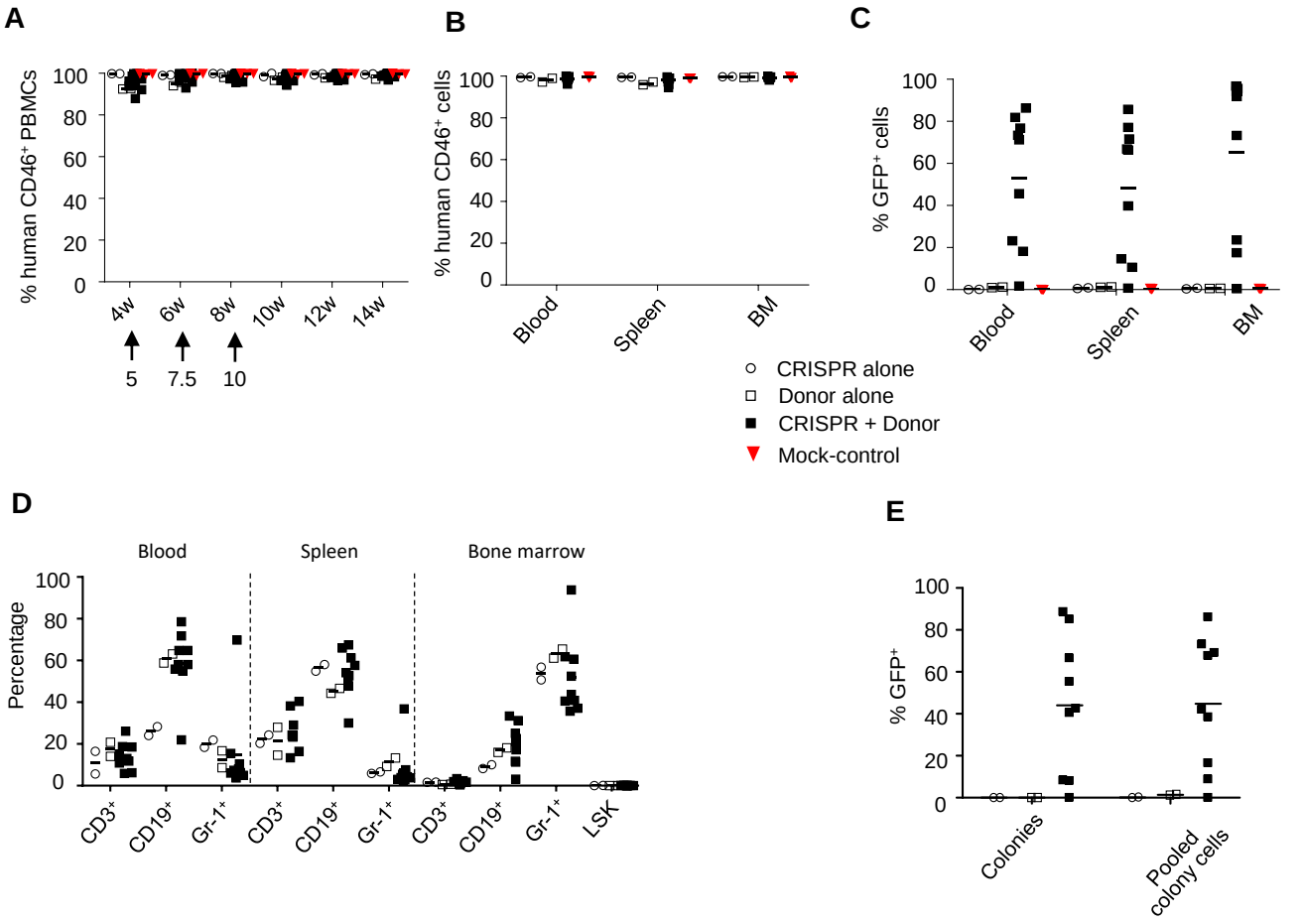

Supplementary Figure S3. Analysis of engraftment of *ex vivo* transduced Lin$^-$ cells. A) Engraftment of transplanted cells based on human CD46 expression in PBMCs measured by flow cytometry. Each symbol is an individual animal. Notably, transduced donor cells expressed CD46, while recipient C57Bl/6 mice did not. N=3 for "CRISPR alone"; N=3 for "Donor alone"; N=10 for "CRISPR+Donor". "Mock-control" are cells that were incubated with the same volume of virus storage buffer (PBS/10% glycerol). **B)** Percentage of CD46-positive cells in PBMCs (blood), spleen, and bone marrow at week 16. **C)** Percentage of GFP-positive cells in PBMCs, spleen and bone marrow, at week 16. **D)** Percentage of LSK and lineage-positive cells. The difference between the three groups is not significant. **E)** Analysis of GFP$^+$ colonies. Total bone marrow Lin$^-$ cells from week 16 mice were plated and GFP expression in colonies was analyzed 12 days later. Each symbol is the average GFP$^+$ colony number for an individual mouse (left panels). Cells from all colonies were pooled and analyzed by flow cytometry (right panels).

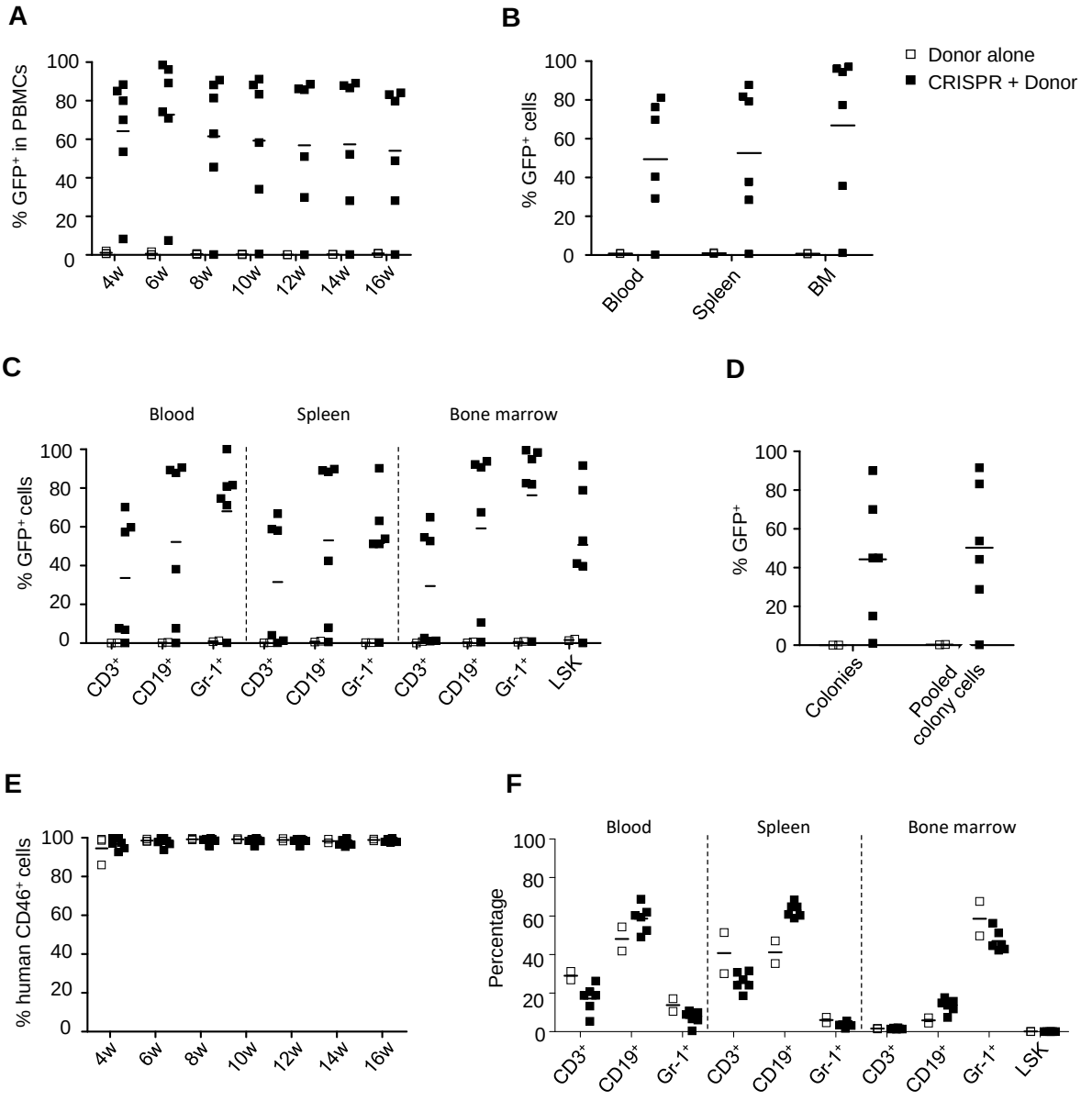

Supplementary Figure S4. Analysis of GFP marking in secondary recipients in the *ex vivo* transduction study (see Fig.3). HDAd-GFP-donor or HDAd-CRISPR + HDAd-GFP-donor transduced Lin$^-$ cells were harvested at week 16 after transplantation, depleted for lineage-positive cells, and transplanted into lethally irradiated C57Bl/6 mice. **A)** GFP expression in PBMCs in recipient mice measured by flow cytometry. N=3 for "Donor alone", N=6 for "CRISPR+Donor". $p<0.01$ **B)** Percentage of GFP-positive cells in PBMCs, spleen and bone marrow at week 16. $p<0.01$. **C)** GFP flow analysis of lineage-positive and LSK cells in recipients 16 weeks after transplantation. $p<0.01$. **D)** Analysis of GFP$^+$ colonies. Total bone marrow Lin$^-$ cells from week 16 mice were plated and GFP expression in colonies was analyzed 12 days later. Each symbol is the average GFP$^+$ colony number for an individual mouse (left panels). Cells from all colonies were pooled and analyzed by flow cytometry (right panels). **E)** Engraftment of transplanted cells based on human CD46 expression on PBMCs measured by flow cytometry. **F)** Percentage of lineage-positive and LSK cells in Donor alone and Donor+CRISPR groups. The difference between the two groups is not significant.

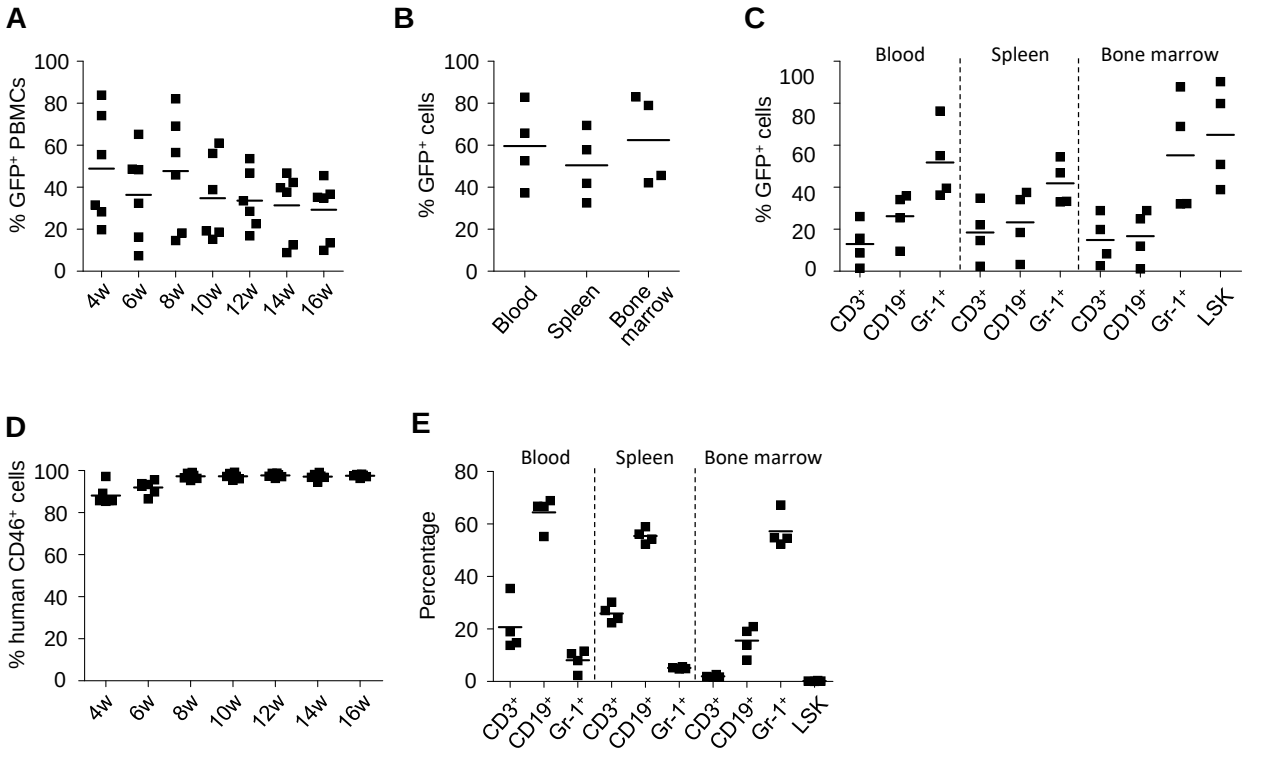

Supplementary Figure S5. Analysis of secondary recipients from Fig.4. At week 14, bone marrow Lin$^-$ cells from *in vivo* transduced AAVS1/hCD46tg mice were transplanted into lethally irradiated C57Bl/6 recipients. **A)** GFP-flow cytometry of PBMCs. N=6. **B)** GFP expression in mononuclear cells in blood, spleen and bone marrow. N=4. **C)** GFP flow analysis of lineage-positive and -negative cells in recipients 16 weeks after transplantation. N=4. **D)** Engraftment of transplanted cells based on human CD46 expression in PBMCs measured by flow cytometry. N=6. **E)** Percentage of lineage-positive and LSK cells at week 16.

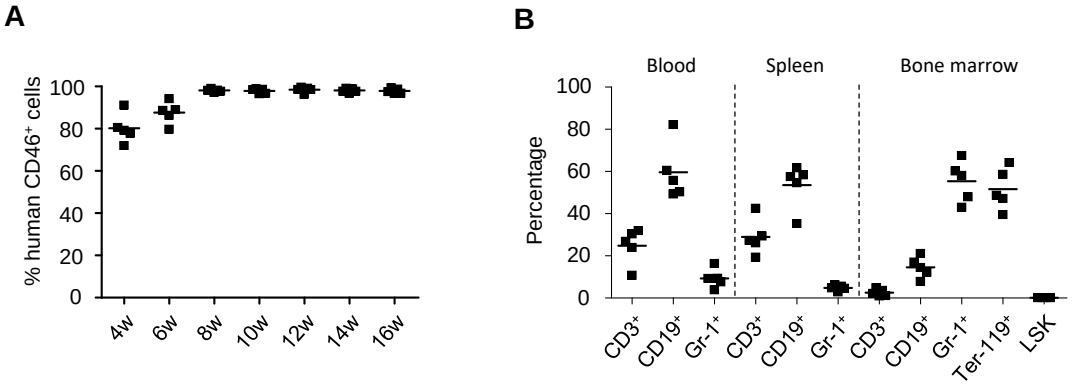

Supplementary Figure S6. Engraftment of AAVS1/CD46 Lin$^-$ cells transduced with HDAd-CRISPR and HDAd-globin-donor vectors. A) Engraftment of transplanted cells based on human CD46 expression on PBMCs measured by flow cytometry. N=5. **B)** Percentage of lineage-positive and LSK cells at week 16. Cells from blood, spleen, and bone marrow were analyzed. N=5.

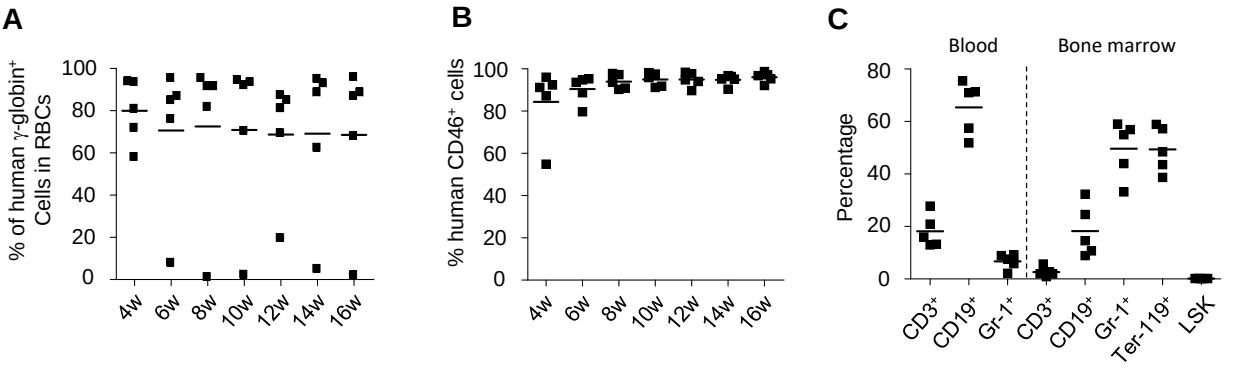

Supplementary Figure S7. Analysis of secondary recipients from Fig. 5. Bone marrow cells from mice that were transplanted with HDAd-CRISPR + HDAd-globin-donor transduced Lin$^-$ cells were harvested at week 16 after transplantation, depleted for lineage-positive cells, and transplanted into lethally irradiated C57Bl/6 mice. N=5. **A)** γ-globin flow cytometry of RBCs in five recipient mice. **B)** Percentage of CD46-positive cells in lineage-positive PBMCs. **C)** Cellular composition in blood (PBMCs) and bone marrow at week 16 after transplantation into secondary recipients. N=5.

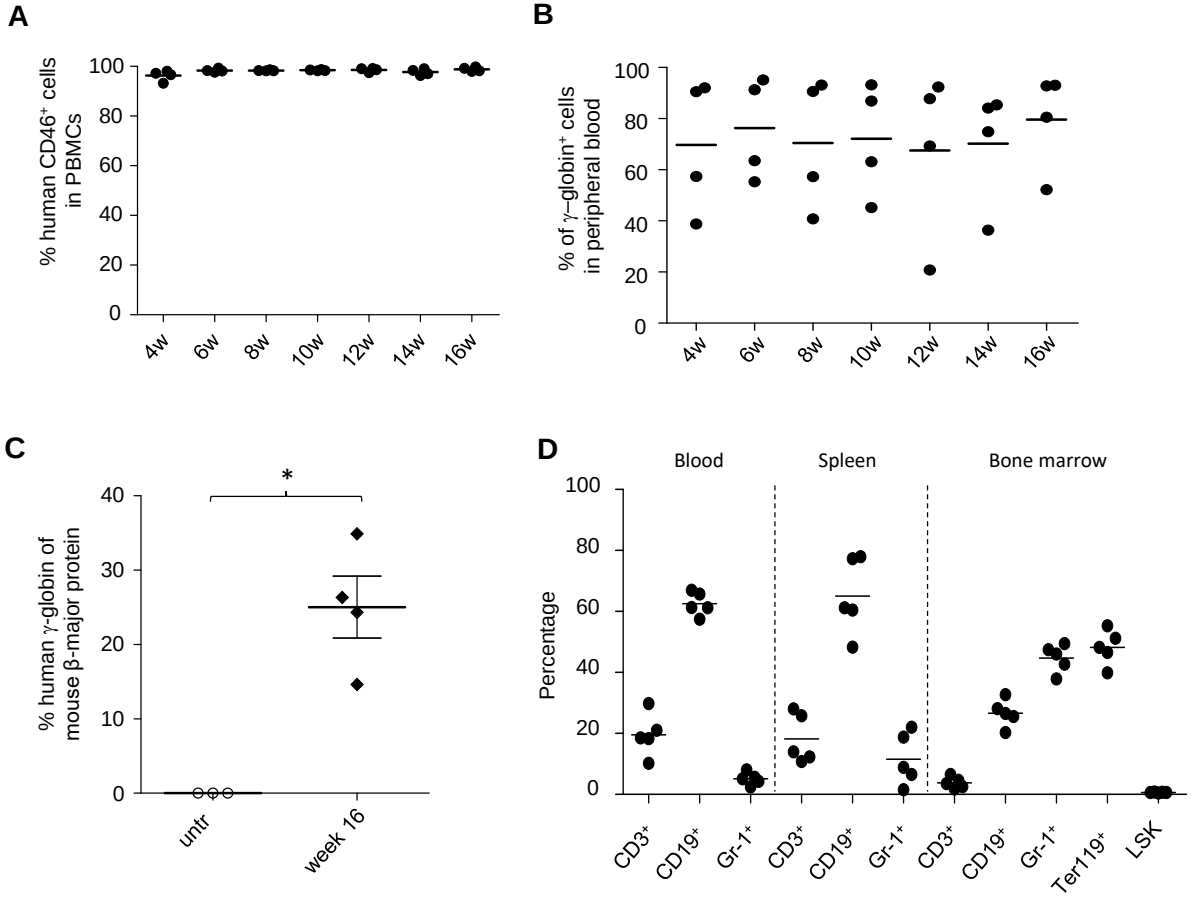

Supplementary Figure S8. Analysis of secondary recipients from Fig.6. At week 16, bone marrow Lin- cells from AAVS1/hCD46tg mice *in vivo* transduced with HDAd-CRISPR + HDAd-globin-donor were transplanted into lethally irradiated C57Bl/6 recipients. N=4. **A)** Engraftment of transplanted cells based on human CD46 expression on PBMCs measured by flow cytometry. **B)** γ-globin expression in RBCs. **C)** Percentage of γ-globin chains relative to mouse beta-major chains measured in RBCs of secondary recipients at week 16 by HPLC. * $p<0.05$. **D)** Lineage-positive and LSK cell composition in blood, spleen and bone marrow at week 16.

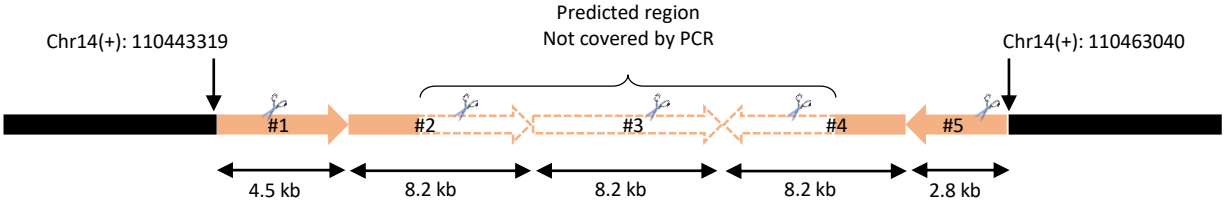

a) One single cut in repeat #1 to #4: preferred
b) One single cut in repeat #5: reduced preference due to incomplete left homology arm
c) Two cuts in two oppositely oriented repeats (e.g. #1 and #4):
no HDR-mediated targeted integration due to missing right homology arm
d) Two cuts in two repeats facing the same direction (e.g. #1 and #2):
preferred
e) For more than 2 cuts, only consider the one proximal to mouse gDNA sequence at each side
Apply rule c) or d) accordingly
f) Cuts in repeats #1 and 5 and deletion of the central region

In addition, if HDR-mediated targeted integration occurred in repeat #2 to #4, continuous cutting in flanking repeats, for example, #1 and #5, by CRISPR may result in loss of the already integrated transgene.

Supplementary Figure S9. Outcome depending on CRISPR/Cas9 cleavage of the multicopy AAVS1 locus present in AAVS1tg mice.

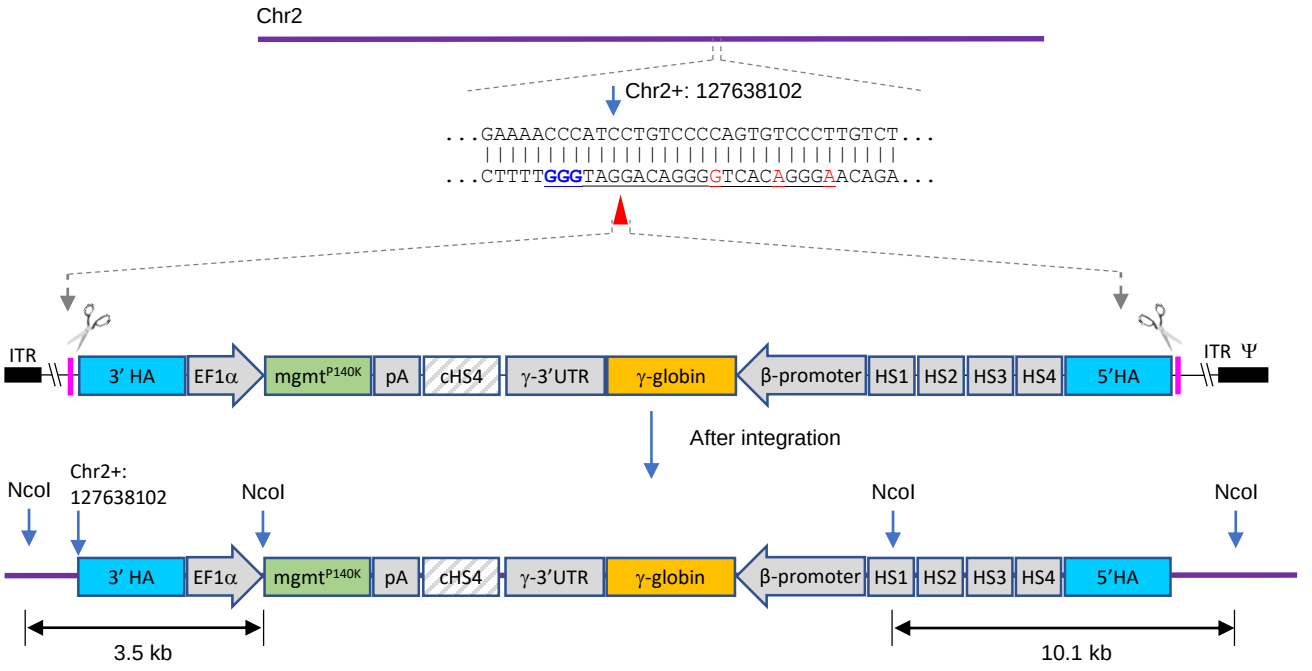

Supplementary Figure S10. Diagram showing CRISPR/Cas9-mediated HDAd-globin-donor integration into an off-target site on chromosome 2. This off-target integration was detected by iPCR in mouse #816. The off-target site Chr2(-): 127638097-127638119 bears 3bp mismatches with the AAVS1 guide sequence. The globin donor cassette (from 5'-HA to 3'-HA) released by AAVS1 CRISPR was reversely integrated into the CRISPR cleavage off-target site (Chr2: 127638102). The location of *NcoI* sites and iPCR amplicon size are indicated.

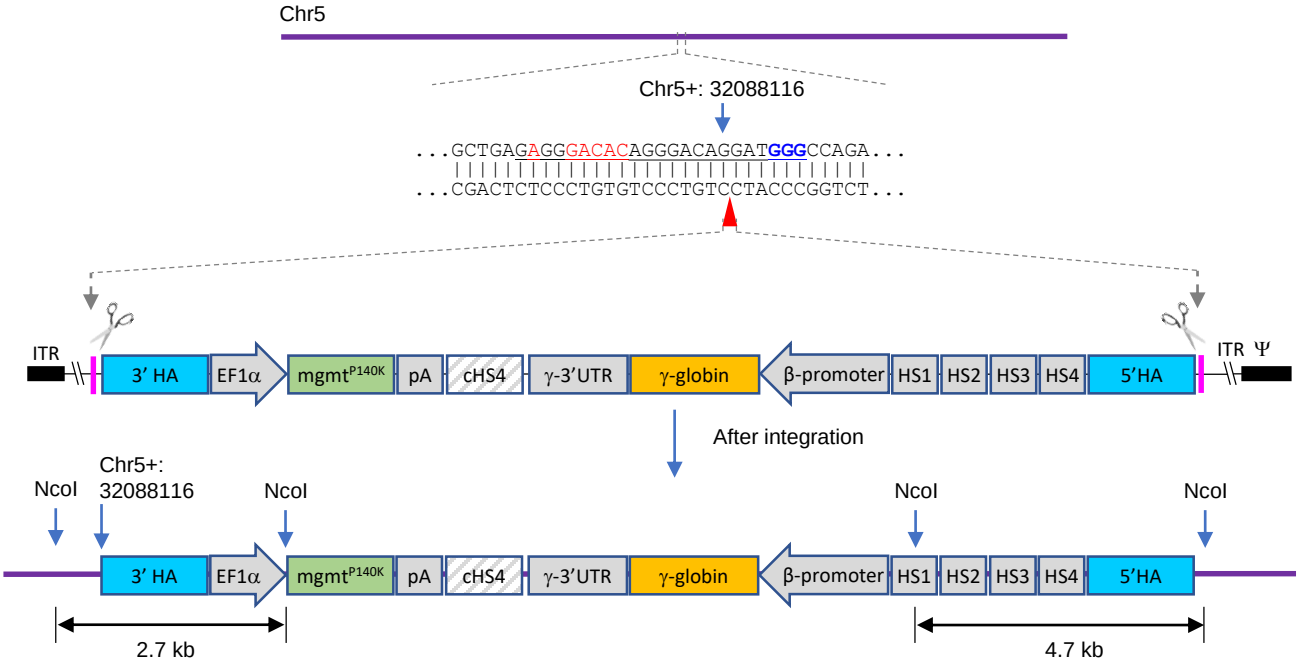

Supplementary Figure S11. Diagram showing CRISPR/Cas9-mediated HDAd-globin-donor integration into an off-target site on chromosome 5. Mice #857 and #945 displayed this off-target integration detected by iPCR. The off-target site Chr5(+): 32088100-32088122 bears 6 bp mismatches with the AAVS1 guide sequence at the PAM-distal side. The globin donor cassette (from 5'-HA to 3'-HA) released by AAVS1 CRISPR was reversely integrated into CRISPR cleavage site (Chr5: 32088116). The location of NcoI sites and iPCR amplicon size are indicated.

mouse #	GFP-donor *(ex vivo)*	γ-globin-donor *(ex vivo)*	GFP-donor *(in vivo)*	γ-globin-donor *(in vivo)*	targeted	off-target	complete HDAd
009	X					X	
023	X				X		
943	X				X		
944	X				X	X	
946	X				X		
147			X		X		
304			X		X		
467			X		X		X
321		X			X		X
322		X			X		
856		X			X		
858		X			X		
945		X			X	X	
504				X	X		
816				X	X	X	
869				X	X		
898				X	X		

Supplementary Figure S12. Summary of integration analyses by iPCR

Supplementary Methods

Generation of HDAd vectors. For the cloning of the HDAd-CRISPR vector, sgRNA (5'-GGGGCCACTAGGGACAGGAT-3') (1) targeting the human AAVS1 locus was synthesized, annealed and inserted into the *BbsI* site of pSPgRNA (Addgene, Cambridge, MA), generating pSP-sgAAVS1. A Cas9 coding sequence amplified from pLentiCRISPRv2 (Addgene), U6sgAAVS1 fragments released by *BamHI* digestion of pSP-sgAAVS1, and a previously described microRNA targeting region (miR-183/218) (2) were sequentially cloned into the *EcoRV-NotI*, *BamHI* and *NotI* sites of pBS-T-EF1α (2), forming pBST-sgAAVS1-miR. To obtain the recombinant adenoviral plasmids, an 8 kb cassette starting from the U6 promoter to the SV40 polyA signal sequence was amplified from pBST-sgAAVS1-miR and ligated with *NheI-XmaI* digested pHCA (3) by Gibson assembly (New England Biolabs), generating the corresponding pHCA-sgAAVS1-miR plasmid.

For the construction of the HDAd-GFP-donor vector, two 0.8kb homology arms (HA) immediately flanking the AAVS1 CRISPR cutting site were synthesized as gBlocks (IDT, San Jose, CA). One 23bp sgAAVS1 with PAM sequence was included upstream of the 5'HA and downstream of 3'HA, respectively, to mediate the release of the donor cassette. A EF1α-mgmt-2A-GFP-pA fragment was synthesized by Genscript (Nanjing, China), and ligated with the two 5'HAs by overlap PCR, forming sgAAVS1-5'HA-Ef1α-mgmt-2A-GFP-pA-3'HA-sgAAVS1 which was subsequently inserted into the *XmaI* site of pHCA (3), generating GFP donor vector pHCA-AAVS1-GFP-mgmt.

The cloning of the HDAd-globin-donor vector involved 3 steps. Step 1) The 11.8kb LCR-globin-mgmt cassette was released from pHM5-FR-IR-LCR-globin-mgmt (4) by *EcoRV-KpnI* digestion and ligated with a 2.8kb plasmid backbone amplified from pBS-Z (2), resulting in pBS-LCR-globin-mgmt. Two 1.8kb HAs immediately adjacent to the AAVS1 CRISPR cutting site were PCR amplified from genomic DNA isolated from bone marrow cells of AAVS1-tg mice using primers containing the 23bp sgAAVS1 with PAM sequence. The 5' and 3' side HAs were sequentially inserted into the *EcoRV* and *KpnI* sites, respectively, of pBS-LCR-globin-mgmt, generating pBS-AAVS1-globin-mgmt. Step 2) The nt1588-12121 region of pHCA was deleted by *EcoRI* digestion and self-ligation, generating pHCAS1. The original *PacI* site in pHCAS1 was destroyed by inserting two annealed oligo sequences. A new *PacI* cloning site was created at the *BstBI* site, getting pHCAS1-MCS. This cloning site was designed in such a way that two 15bp homologous regions will be exposed upon *PacI* digestion. The size of pHCAS1-MCS was further reduced by removing the 1.5kb *NheI* fragment, resulting in pHCAS1S-MCS. Step 3) Following *PacI* digestion of the two final constructs from the above two steps, the products were recombined by Gibson Assembly, generating the globin donor vector pHCA-AAVS1-globin-mgmt.

Next generation sequencing. For deep sequencing of insertion/deletions (indels), we PCR-amplified a ~250-bp region surrounding the predicted AAVS1 cleavage site and sequenced the products using an Illumina system. Genomic DNA was isolated as previously described (2). A 249 bp genomic region encompassing the AAVS1 target site was amplified using the following primers: AAVS1 forward, 5'-CGGTTAATGTGGCTCTGGTT-3'; reverse, 5'-CCTCTCTGGCTCCATCGTAA-3'. After cleaning-up the amplicon using AMPure XP Beads (Beckman Coulter, Indianapolis, IN), dA-tailing was performed using Klenow fragment. Illumina-compatible adaptors were ligated with the product by T4 ligase (New England Biolabs). A unique barcode sequence was introduced by PCR to allow sequencing multiple samples on the same sequencing run. Each step was followed by purification with AMPure XP Beads. The final libraries were quantified by Qubit (Invitrogen) and tested on an Agilent 2100 Bioanalyzer to determine average size of the amplicons. The amplicons were pooled at equal molarity and deep sequenced on an Illumina MiSeq system. Approximately 10^5 reads per amplicon were generated to adequately probe the types of mutations. Sequencing data were aligned to the AAVS1 reference sequence using the Cas-Analyzer online

tool (http://www.rgenome.net/cas-analyzer/#!) (5), a JavaScript-based implementation for NGS data analysis.

Flow cytometry: Cells were resuspended at 1×10^6 cells/100 μL in FACS buffer (PBS supplemented with 1 % heat-inactivated FBS) and incubated with FcR blocking reagent (Miltenyi Biotech, Auburn CA) for ten minutes on ice. Next the staining antibody solution was added in 100 μL per 10^6 cells and incubated on ice for 30 minutes in the dark. After incubation, cells were washed once in FACS buffer. For secondary staining the staining step was repeated with a secondary staining solution. After the wash, cells were resuspended in FACS buffer and analyzed using a LSRII flow cytometer (BD Biosciences, San Jose, CA). Debris was excluded using a forward scatter-area and sideward scatter-area gate. Single cells were then gated using a forward scatter-height and forward scatter-width gate. Flow cytometry data were then analyzed using FlowJo (version 10.0.8, FlowJo, LLC). For flow analysis of LSK cells, cells were stained with biotin-conjugated lineage detection cocktail (Miltenyi Biotec, San Diego, CA) and antibodies against c-Kit and Sca-1 as well as APC-conjugated streptavidin. Other antibodies from eBioscience (San Diego, CA) included anti-mouse LY-6A/E (Sca-1)-PE-Cyanine7 (clone D7), anti-mouse CD117 (c-Kit)-PE (Clone 2B8), anti-mouse CD3-APC (clone 17A2), anti-mouse CD19-PE-Cyanine7 (clone eBio1D3), and anti-mouse Ly-66 (Gr-1)-PE, (clone RB6-8C5). Other antibodies from Miltenyi Biotec included anti-human CD46-APC (clone: REA312). Anti-mouse Ter-119-APC (clone: Ter-119) was from Biolegend (San Diego, CA).
Intracellular staining of human γ-globin was performed using PE-conjugated anti-human γ-globin antibody from Santa Cruz (clone 51.7). The Fix & Perm cell permeabilization kit from Invitrogen was used according to manufacturer's instructions.

Inverse PCR*:* Junctions in total bone marrow cells, single colonies, HUDEP-2 cell mixture or clones were analyzed by inverse PCR as described elsewhere with modifications (6). Briefly, genomic DNA was isolated by incubating with genomic DNA lysis buffer (100 mM Tris-Cl (pH 8.0), 50 mM EDTA, 1% (w/v) SDS, and 400 μg/mL Proteinase K) at 55°C overnight with shaking, followed by phenol-chloroform extraction, precipitation with isopropanol, and wash with 70% ethanol. The DNA samples were dissolved in 10 mM Tris/HCL buffer (pH 8.5). 5 μg of DNA was digested with 30 U *NcoI* in 50 μL reaction at 37°C for 5 hours. After heat-inactivation and clean-up, the digested DNA was treated with 2.5 μL T4 ligase (New England Biolabs, M0202L) in 500 μL reaction buffer at 16°C overnight for intramolecular ligation. Following heat-inactivation and clean-up, the religated product was used for inverse PCR using KOD Hot Start DNA Polymerase. The following primers were used: EF1α forward, 5'-AACAAAAGCTGGTTAATTAAATCGGACGGGGGTAGTCTCAAG-3', and reverse, 5'-TATTGTACCATCTTAATTAAAGGGGCGAGTCCTTTTGTATG-3'; pA forward, 5'-AACAAAAGCTGGTTAATTAATCATTTTATGTTTCAGGTTCAGGGGG-3', and reverse, 5'-TATTGTACCATCTTAATTAAATGGTTACAAATAAAGCAATAGCATCAC-3'; HS4 forward, 5'-AACAAAAGCTGGTTAATTAAGTTTTTGTATTCTGTTTCGTGAGGCA-3'; and reverse, 5'-TATTGTACCATCTTAATTAAGCATTTGCCTAAGGTCGGACAT-3'. The underlined bases are *PacI* sites used for downstream cloning. The Ef1α and pA primer pairs were used for analyzing 5' and 3' junctions of GFP donor vector-treated samples, respectively. The HS4 and EF1α primer pairs were used for analyzing 5' and 3' junctions of globin donor vector-treated samples, respectively. PCR amplicons were gel purified, cloned, sequenced and aligned to identify the integration sites.
In-Out PCR: Genomic DNA was extracted as described in the section of Inverse PCR. 5 ng genomic DNA was directly used as template for In-Out PCR by KOD Hot Start DNA Polymerase in a 25 μl of reaction. The following PCR program was used: 94°C 2 min; 5 cycles of 98°C 10 sec, 66°C 30 sec and 68°C 1.5 min; 5 cycles of 98°C 10 sec, 63°C 30 sec and 68°C 1.5 min; 15 cycles of 98°C 10 sec, 60°C 30 sec and 68°C 1.5 min; 68°C 5min. Primers used are In-Out P1, 5'-CCACACCCAGACCTGACCCAAACC-3', In-Out P2, 5'-CGGGAACCACACACGGCACTTACC-3', and In-Out P3, 5'-TCTAACGCTGCCGTCTCTCTCCTG-3'. The products

were resolved in a 1% Agarose gel. One single 1.6 kb band indicates biallelic targeted integration; one 1.6 kb plus one 2.0 kb band indicates monoallelic targeted integration; one single 2.0 kb band indicates potential off-target integration.

References:

1. Mali, P., Yang, L., Esvelt, K.M., Aach, J., Guell, M., DiCarlo, J.E., Norville, J.E. and Church, G.M. (2013) RNA-guided human genome engineering via Cas9. *Science*, **339**, 823-826.
2. Saydaminova, K., Ye, X., Wang, H., Richter, M., Ho, M., Chen, H., Xu, N., Kim, J.S., Papapetrou, E., Holmes, M.C. *et al.* (2015) Efficient genome editing in hematopoietic stem cells with helper-dependent Ad5/35 vectors expressing site-specific endonucleases under microRNA regulation. *Mol Ther Methods Clin Dev*, **1**, 14057.
3. Sandig, V., Youil, R., Bett, A.J., Franlin, L.L., Oshima, M., Maione, D., Wang, F., Metzker, M.L., Savino, R. and Caskey, C.T. (2000) Optimization of the helper-dependent adenovirus system for production and potency in vivo. *Proc Natl Acad Sci U S A*, **97**, 1002-1007.
4. Li, C., Psatha, N., Wang, H., Singh, M., Samal, H.B., Zhang, W., Ehrhardt, A., Izsvak, Z., Papayannopoulou, T. and Lieber, A. (2018) Integrating HDAd5/35++ Vectors as a New Platform for HSC Gene Therapy of Hemoglobinopathies. *Mol Ther Methods Clin Dev*, **9**, 142-152.
5. Park, J., Lim, K., Kim, J.S. and Bae, S. (2017) Cas-analyzer: an online tool for assessing genome editing results using NGS data. *Bioinformatics*, **33**, 286-288.
6. Wang, H., Shayakhmetov, D.M., Leege, T., Harkey, M., Li, Q., Papayannopoulou, T., Stamatoyannopolous, G. and Lieber, A. (2005) A capsid-modified helper-dependent adenovirus vector containing the beta-globin locus control region displays a nonrandom integration pattern and allows stable, erythroid-specific gene expression. *J Virol*, **79**, 10999-11013.